UNIVERSITY OF CAMBRIDGE | Energy Policy Research Group

Marginal curtailment under network constraints: evidence from the 2030 GB power system

Chi Kong Chyong[1] and David Newbery[2]

EPRG Working Paper **EPRG2524**

Cambridge Working Paper in Economics **CWPE2581**

Abstract

High Variable Renewable Electricity (VRE) penetration inevitably leads to curtailment (shedding), typically measured by average curtailment. Marginal curtailment (mc, the fraction of potential output curtailed by the last MW) can be many times higher, raising the long-run marginal cost of investment, proportional to 1/(1-mc). A unit commitment and economic dispatch model of Britain, divided into seven zones by transmission constraints in 2030, demonstrates that these constraints considerably increase mc compared to no congestion, despite the considerable planned expansion of transmission, interconnectors, and storage that mitigates curtailment. The current auction design favours levelised costs, ignoring curtailment, but long-run marginal costs may be 90% higher, suggesting the need for careful locational planning and VRE support design.

Keywords Variable Renewable Electricity, Marginal Curtailment, Average Curtailment, Levelised Cost of Electricity, VRE support design.

JEL Classification L94; Q28; Q42; Q48

Contact David Newbery, dmgn@cam.ac.uk
Energy Policy Research Group,
Faculty of Economics,
University of Cambridge,
Sidgwick Ave., Cambridge,
CB3 9DD, UK

[1] Oxford Institute for Energy Studies, 57 Woodstock Road, Oxford OX2 6FA. kong.chyong@oxfordenergy.org
[2] dmgn@cam.ac.uk, Faculty of Economics, University of Cambridge, Sidgwick Ave. Cambridge CB3 9DD.

Marginal curtailment under network constraints: evidence from the 2030 GB power system

Chi Kong Chyong[1] and David Newbery[2]

Version 30 January 2026

Abstract

High Variable Renewable Electricity (VRE) penetration inevitably leads to curtailment (shedding), typically measured by average curtailment. Marginal curtailment (*mc*, the fraction of potential output curtailed by the last MW) can be many times higher, raising the long-run marginal cost of investment, proportional to 1/(1-*mc*). A unit commitment and economic dispatch model of Britain, divided into seven zones by transmission constraints in 2030, demonstrates that these constraints considerably increase *mc* compared to no congestion, despite the considerable planned expansion of transmission, interconnectors, and storage that mitigates curtailment. The current auction design favours levelised costs, ignoring curtailment, but long-run marginal costs may be 90% higher, suggesting the need for careful locational planning and VRE support design.

Key words: Variable Renewable Electricity, Marginal Curtailment, Average Curtailment, Levelised Cost of Electricity, VRE support design.

1. Introduction

Electricity systems in most countries are undergoing rapid expansion of variable renewable electricity (VRE), particularly wind and solar photovoltaic generation. This reflects both decarbonisation policies and the sustained decline in the cost of these technologies, which has brought new renewables into closer competition with fossil generation once carbon costs are factored in. As VRE penetration rises, curtailment becomes more common. When demand, storage, and export opportunities are saturated, surplus output has limited value and must be spilled.

Recent work shows that curtailment is not solely determined by VRE penetration. It also depends on the composition of VRE technologies and on where they are located. Newbery and Chyong (2025) show that expanding one VRE technology, for example, onshore wind, can increase curtailment of other technologies, including offshore wind and solar PV, because their output profiles differ across hours. In such settings, marginal curtailment, the curtailment associated with an incremental unit of capacity, can be far above average curtailment. This divergence is particularly strong in systems with multiple VRE technologies, compared with systems dominated by a single resource such as the island of Ireland, which has a high share of onshore wind (Newbery, 2023).

We extend that analysis by focusing on the role of internal transmission constraints. Where internal boundaries bind, additional VRE capacity affects not only local balancing but also

[1] Corresponding author; Oxford Institute for Energy Studies, 57 Woodstock Road, Oxford OX2 6FA. kong.chyong@oxfordenergy.org

[2] Faculty of Economics, University of Cambridge, Sidgwick Ave., Cambridge CB3 9DE. dmgn@cam.ac.uk

interzonal flows and the curtailment of neighbouring regions. The resulting spillovers raise marginal curtailment for both new and existing generation. In turn, they increase the long-run marginal cost of investment in constrained areas even when average curtailment remains relatively modest. In this setting, curtailment is not simply a feature of technology and temporal coincidence; network constraints and the spatial pattern of investment also shape it.

These issues are closely linked to the legacy structure of transmission networks. Most systems were built around large, centralised fossil and nuclear stations and designed to deliver power to load centres. VRE, by contrast, is typically located where resources are strongest, often distant from demand. As deployment has accelerated, internal and inter-regional congestion has become more frequent, prompting the need for network reinforcement mechanisms to better guide investment and operation across space. In Great Britain (GB), these concerns were a central motivation for the Review of Electricity Market Arrangements (REMA) launched in 2022 (HMG, 2022).

A key feature of this transition is the widening gap between average and marginal curtailment. Average curtailment is the metric most commonly reported by system operators and planners, but marginal curtailment is what governs the economics of incremental investment. Where transmission capacity is poorly aligned with the emerging spatial pattern of generation and demand, marginal curtailment can exceed average curtailment by a wide margin. That has direct implications for both policy and investment, because it strengthens the case for more explicit locational guidance to avoid further concentration of capacity behind already constrained boundaries.

Congestion can be managed through a mix of better siting of new generation, improved utilisation of existing assets, and long-term transmission investment. In GB, the National Energy System Operator, NESO, has been tasked with strategic spatial energy planning. These measures are necessary, but we emphasise a complementary point: when binding internal constraints are present, VRE investments should be assessed using marginal rather than average delivered costs. As we show below, the marginal cost of delivered VRE increases non-linearly with marginal curtailment, scaling as $1/(1-mc)$, where mc denotes marginal curtailment (as a share of potential output).

In systems where investment decisions are decentralised, the relevance of these cost differences depends on whether they are visible to investors. In liberalised electricity markets, the siting of new capacity is guided by prices, network charges, and the design of renewable support schemes rather than by central allocation. Internal constraints must be respected in dispatch regardless of the pricing regime, such as national, zonal or locational marginal pricing. However, the extent to which curtailment risk is reflected in revenues and support payments depends on the degree of spatial price aggregation and on contract design. When marginal curtailment differs sharply across locations but is not reflected in commercial incentives, investment can be steered towards high-resource areas even when the delivered-value penalty from congestion dominates. What has been missing from much of the policy debate and from much applied economic modelling is a systematic measurement of how marginal curtailment varies across space in constrained systems and what that implies for location-specific long-run marginal costs of renewable investment.

We address that gap by quantifying average and marginal curtailment across zones in a power system with binding internal transmission constraints and by deriving location-specific long-run marginal costs for wind and solar generation. Using a 2030 GB electricity market as a detailed case study, we show how internal constraints translate into sharp differences in marginal delivered costs across space, and we discuss the implications for aligning pricing and support arrangements with efficient renewable deployment in liberalised electricity markets more broadly. The article is structured as follows: we review the literature in the next section; present our research framework in Section 3, Sections 4 and 5 report modelling results and implications for long-run marginal costs; policy implications are presented in Section 6 and conclusions in Section 7.

2. Literature review

The rapid expansion of wind and solar has brought renewed attention to whether electricity market arrangements provide sufficiently clear spatial signals for efficient investment and system operation. As VRE deployment increases, congestion and curtailment are increasingly determined by where generation is built relative to demand and network capacity. Much of the academic and policy literature still treats these outcomes in highly aggregated terms. Curtailment is typically reported as a system-level average, even though the economics of further investment depend on marginal curtailment: the additional curtailment caused by an incremental increase in capacity in a particular location. Compared with average curtailment, marginal curtailment has received much less systematic treatment, despite being the relevant metric for the viability of new projects in constrained parts of the system.

Early work on renewable curtailment often abstracted from internal transmission constraints. Newbery (2021), for example, examined wind curtailment in the Single Electricity Market in the island of Ireland under frequency-stability constraints but did not model internal system bottlenecks. Simshauser and Newbery (2024) analysing a Renewable Energy Zone in Queensland, show that when export limits bind, marginal curtailment considerably exceeds average curtailment. Newbery and Chyong (2025) extend this logic to a multi-technology setting in simulations of a future GB power system. Under a copper-plate representation with export constraints but without internal transmission limits, they report marginal-to-average curtailment ratios in the range of five to seven. The implication is that even without internal congestion, the relationship between renewable penetration and the marginal cost of additional clean generation can be strongly non-linear.

In parallel, a large empirical and modelling literature evaluates how spatial price granularity - typically zonal pricing or locational marginal pricing (LMP) - affects dispatch efficiency and, in some cases, investment incentives. On dispatch efficiency, evidence from markets that have adopted nodal pricing points shows measurable operational efficiency gains. In ERCOT, Zarnikau et al. (2014) report that nodal pricing reduced average wholesale prices paid by load-serving entities by around 2-3%. Triolo and Wolak (2022) estimate a 3.9% reduction in thermal generation costs, translating into annual savings exceeding USD 300 million. Wolak (2011) documents a 2.5% reduction in fuel consumption for gas-fired generation following the introduction of nodal pricing in California. While these contributions establish that dispatch outcomes can improve with greater spatial granularity they say less about how

curtailment evolves across pricing regimes or, the far more important issue of how spatial pricing affects the economics of incremental renewable investment.

In the same vein, European contributions tend to focus on zonal pricing and the configuration of bidding zones for existing generation. Using data and scenarios associated with ENTSO-E's Bidding Zone Review, Bichler et al. (2025) simulate alternative zonal arrangements for Germany and find only modest system-wide dispatch efficiency gains. Dobos et al. (2025) similarly conclude that data-driven zone proposals deliver limited and unstable improvements in congestion management. In the Swedish context, Loiacono et al. (2025) find clearer price differentiation in constrained southern regions, but relatively small effects on aggregate efficiency. Thus, this strand of work suggests that the main step-change in dispatch efficiency comes from moving away from a single national price where congestion is material; beyond that, the benefits of further refinement depend on the extent to which internal congestion becomes persistent as VRE penetration increases.

The more important (in terms of system cost) literature examines investment responses and curtailment outcomes under different degrees of spatial price differentiation. Ambrosius et al. (2020), using a multilevel optimisation model of the German market, find that optimally defined price zones can reduce renewable curtailment and redirect investment across technologies. Katzen and Leslie (2024) provide empirical evidence from Australia that zonal pricing can encourage siting behind constraints, with observed curtailment rates of 4.4% for wind and 4.7% for solar - levels they argue would likely be lower under nodal pricing. Also in Australia Newbery and Biggar (2024) showed that if VRE developers pay the full cost of connecting to an unconstrained system, accepting unremunerated curtailment allocated in proportion to offers leads to efficient sizing of transmission and VRE investment. Lundin (2022) finds that Sweden's zonal reform induced developers to reallocate around 18% of planned wind projects towards higher-priced zones, indicating that investment can respond to spatial price differentials when these are sufficiently salient.

More recent work also highlights the interaction between spatial pricing and demand-side flexibility. Using a high-resolution European model, Boehnke et al. (2025) show that nodal pricing reveals localised "flexibility hot spots", where distributed storage, electric vehicles and heat pumps deliver higher system value than under zonal pricing. Lyden et al. (2024) report analogous findings for Great Britain, showing that locational pricing changes the operating cost of heat pumps across regions and can influence where electrified heat is deployed. Kenis et al. (2024) extend the argument to hybrid offshore wind and hydrogen production, finding that nodal pricing can reduce curtailment and increase welfare when flexible demand is co-located with generation. The broader point is that spatial price granularity has implications beyond generation dispatch: it can shape the location and value of flexibility resources that mitigate curtailment.

The welfare implications of granular pricing have been examined in both theoretical and applied settings. Green (2007) estimates that nodal pricing in a stylised GB system could increase welfare by around 1.3% of generator revenues. Neuhoff et al. (2013), using a European network model, find that nodal pricing can increase cross-border flows by 34% and reduce operating costs by up to EUR 2 billion per year. Aravena and Papavasiliou (2016)

compare nodal and zonal coordination mechanisms and show that zonal designs can lead to higher balancing and redispatch costs, particularly when forecast errors are material, which is directly relevant in systems with high shares of wind and solar.

Despite the breadth of this literature, two central gaps remain. First, curtailment is still most often analysed as an average or aggregate outcome rather than as a marginal object linked to incremental investment in specific locations. Second, even when studies compare uniform, zonal, and nodal pricing in terms of dispatch efficiency or welfare, they rarely examine how binding internal transmission constraints reshape marginal curtailment and, through that channel, alter long-run investment incentives. These limitations are also visible in applied modelling and planning work,[3] which often reports total curtailed volumes or constraint costs but does not quantify marginal curtailment or translate it into the long-run marginal cost of renewable deployment (Oree et al., 2017; Koltsaklis and Dagoumas, 2018; Dagoumas and Koltsaklis, 2019; van Ouwerkerk et al., 2022). This matters for market design and support-scheme calibration, where marginal metrics serve as the basis for assessing the cost of additional capacity in constrained areas.

We contribute to this literature by explicitly computing both average and marginal curtailment in a system with binding internal transmission constraints, and by documenting how marginal curtailment varies across technologies and locations. We then translate these estimates into location-specific long-run marginal costs of wind and solar investment, linking curtailment dynamics directly to the investment problem faced in liberalised markets. In doing so, we shift attention from average outcomes and aggregate efficiency comparisons to the marginal, location-specific costs that sit at the centre of efficient renewable deployment when congestion is persistent.

3. Research framework

3.1 A stylised dispatch framework, marginal curtailment, and cost metrics

To make the role of internal transmission constraints transparent, we use a stylised linear dispatch problem that reproduces the feasibility logic of a standard unit commitment and economic dispatch (UCED) model (for detailed mathematical formulation of the UCED model, see Appendix 3 and for data inputs and assumption see Appendix 1), while abstracting from unit commitment binaries and other operational details that are not needed for the curtailment results that follow.

Consider a power system comprising a set of zones $z \in Z$, connected by transfer-constrained internal boundaries, and operating over a set of hours $h \in H$. Variable renewable electricity (VRE) generation is indexed by technology $i \in I$, where I={onshore wind, offshore wind, solar PV}. Dispatchable generation technologies are indexed by $j \in J$.

[3] See, e.g., consulting studies commissioned to inform the GB Review of Electricity Market Arrangements (REMA). These consulting studies provide valuable system-specific insight on the potential impacts of spatial pricing reform. Studies by FTI Consulting (2023, 2025), AFRY (2025a, b), Aurora (2023), Frontier Economics & LCP Delta (2024), and LCP Delta (2024) model various zonal and national pricing scenarios, primarily using dispatch and investment models calibrated to GB's network and capacity plans.

For each technology, zone and hour, the potential VRE output $\bar{w}_{izh}$ is exogenously given by installed capacity and weather conditions. Actual realised VRE generation w_{izh} may be lower than potential output due to system constraints, with the difference interpreted as curtailment. Dispatchable generation g_{izh}, interzonal power flows $f_{z\to k,h}$ and (where relevant) storage operations ensure hourly balance. The system is represented by the following constraints.

VRE availability and curtailment: $0 \le w_{izh} \le \bar{w}_{izh}, c_{izh} \equiv \bar{w}_{izh} - w_{izh}$, where c_{izh} denotes curtailment of technology i in zone z during hour h.

Zonal power balance: $\sum_j g_{jzh} + \sum_i w_{jzh} + \sum_k f_{k\to z,h} = d_{zh} + \sum_k f_{z\to k,h}$, where d_{zh} denotes electricity demand in zone z and hour h. Storage charging and discharging can be included without loss of generality, but are omitted here for expositional clarity.

Internal transmission constraints: $0 \le f_{z\to k,h} \le \bar{F}_{zk}$, where $\bar{F}_{zk}$ denotes the transfer capacity of the internal boundary between zones z and k.

Dispatchable generation bounds: $0 \le g_{jzh} \le \bar{g}_{jz}$, with $\bar{g}_{jz}$ denoting installed capacity.

Additional system-wide feasibility constraints: in particular, high penetrations of inverter-based generation often require limits on instantaneous VRE output to maintain frequency stability. This can be represented by a system stability constraint of the form:

$$\sum_z \sum_i w_{izh} \le \alpha \left(\sum_z d_{zh} + exports_h + storage\ charging_h \right),$$

where $\alpha \in (0, 1)$ captures the maximum share of VRE compatible with secure operation.

Given these constraints, the system operator selects feasible dispatch and flows to minimise short-run system cost:

$$min \sum_{h,z,i,j} v_j g_{jzh} + v_i w_{izh} ,$$

where v_j denotes the variable cost of dispatchable technology j. Curtailment arises implicitly as the residual required to maintain feasibility when potential VRE output exceeds what can be absorbed locally or exported through the network.

This formulation highlights three properties that are central to the subsequent analysis. First, curtailment arises endogenously as a feasibility outcome rather than as an exogenous assumption. Second, curtailment is location- and technology-specific, reflecting both the spatial distribution of VRE potential and the configuration of internal transmission constraints. Third, and most importantly for this article, the optimal curtailment response to a marginal increase in VRE potential in a given zone depends critically on whether internal transfer constraints are binding in the relevant hours. This dependence is explored formally in the next subsection through the definition and measurement of marginal curtailment.

Curtailment is measured as the fraction of potential VRE output that cannot be accommodated by the system. For each technology i, zone z, and hour h, curtailment is

defined as: $c_{izh} \equiv \bar{w}_{izh} - w_{izh}$. Aggregating over time yields total curtailment $C_{iz} = \sum_h c_{izh}$ and total potential output $\bar{W}_{iz} = \sum_h \bar{w}_{izh}$. Average curtailment is then given as

$$ac_{iz} = \frac{C_{iz}}{\bar{W}_{iz}}$$

This statistic describes the fraction of potential output lost for the existing fleet. It is widely reported, but it is not appropriate for incremental investment appraisal. We measure marginal curtailment by applying a small proportional increase in the potential output of technology i in zone z,

$$\bar{w}'_{izh} = (1 + \varepsilon)\bar{w}_{izh},$$

and computing the resulting changes in total curtailment ΔC_{iz} and potential output $\Delta \bar{W}_{iz}$. Marginal curtailment is

$$mc_{iz} = \frac{\Delta C_{iz}}{\Delta \bar{W}_{iz}}$$

The distinction between ac_{iz} and mc_{iz} is central to the analysis. When curtailment arises primarily in a limited subset of hours, such as periods when system-wide stability limits (SNSP) bind or when internal transmission constraints are congested, additional capacity is disproportionately curtailed. In such cases, marginal curtailment can substantially exceed average curtailment, reflecting the non-linear interaction between new VRE output and binding constraints.

Curtailment directly affects the effective utilisation of installed capacity and therefore the cost of delivered electricity. Let PCF_{iz} denote the potential capacity factor of technology i in zone z, defined as potential output per unit of installed capacity. Average and marginal capacity factors are then given by

$$ACF_{iz} = (1 - ac_{iz})PCF_{iz}, \quad (1)$$

$$MCF_{iz} = (1 - mc_{iz})PCF_{iz}. \quad (2)$$

The standard levelised cost of electricity (LCoE) is defined as

$$LCoE_{iz} = \frac{F_i}{8760 \cdot PCF_{iz}} + v_{i,}$$

where F_i denotes the annualised fixed cost per unit of capacity (including capital recovery and fixed operating costs) and v_i the variable operating cost, both in £/MWh. This measure implicitly assumes that all potential output is delivered.

When curtailment is present, the relevant cost metrics differ. The levelised average cost of delivered electricity is

$$LACoE_{iz} = \frac{F_i}{8760 \cdot ACF_{iz}} + v_i = \frac{LCoE_{iz} - v_i}{1 - ac_{iz}} + v_i, \quad (3)$$

while the levelised marginal cost of delivered electricity associated with an incremental capacity addition is

$$LMCoE_{iz} = \frac{F_i}{8760 \cdot MCF_{iz}} + v_i = \frac{LCoE_{iz} - v_i}{1 - mc_{iz}} + v_i. \quad (4)$$

For technologies with low (wind) or zero (PV) variable operating costs these expressions simplify to

$$LACoE_{iz} \approx \frac{LCoE_{iz}}{1 - ac_{iz}}, \qquad LMCoE_{iz} \approx \frac{LCoE_{iz}}{1 - mc_{iz}}.$$

The amplification factors 1/(1-ac_{iz}) and 1/(1-mc_{iz}) provide a convenient metrics for how curtailment inflates average and marginal costs.

Because marginal curtailment can be several times larger than average curtailment, the divergence between $LACoE_{iz}$ and $LMCoE_{iz}$ can be substantial. This implies that investment decisions guided by average curtailment or headline LCoE figures may significantly understate the actual cost of expanding VRE capacity in constrained locations. The rest of this article focuses on identifying mc_{iz} and the associated $LMCoE_{iz}$ using a detailed UCED model that captures the interaction between temporal VRE profiles, internal transmission constraints, external export capability, storage and system-wide feasibility constraints (SNSP).

3.2 UCED implementation, data, and scenario design

The analytical framework set out in Section 3.1 is implemented using a detailed Pan-European UCED model. The model extends the framework developed by Chyong and Newbery (2022) and captures the interactions among high-resolution temporal variability in VRE output, internal transmission constraints, external trade, system-wide feasibility limits and hydrogen production.

3.2.1 Spatial and temporal resolution

The model represents 19 European electricity systems, with Great Britain modelled at a finer spatial resolution to explicitly capture internal congestion. GB is divided into seven zones (Z1-Z7), separated by transfer-constrained internal boundaries selected to reflect persistent and material transmission bottlenecks. These zonal boundaries are illustrated in Figure 1, and the associated directional transfer capacities for 2023 and 2030 are reported in Table 1.

Figure 1: Zonal boundaries selected for zonal pricing experiments

From	To	Boundary	2023 cap.	2030 cap.	IC*	To
Z1	**Z2**	B4	4,000	7,300	0	
Z2	**Z3**	B6	6,700	10,200	450	SEM
Z3	**Z4**	B7a	9,400	13,500	1,464	NO
Z4	**Z5**	B8	11,000	16,400	500	SEM
Z5	**Z6**	EC5	3,300	13,500	7,100	BE, DE, DK, NL, SEM, FR
Z5	**Z7**	SC1	3,900	6,100	5,000	BE,FR

* IC - external interconnectors

Table 1: Transfer capacity (MW) in 2023 and 2030, and 2030 export capacity (MW)
Source: ESO (2024) and Appendix 1

Internal transmission constraints limit flows across boundaries such as B4, B6, B7a, B8, EC5, and SC1. Zones are also connected to external systems via aggregated interconnector capacities that limit trade with neighbours (e.g. SEM, Norway, Belgium, France, the Netherlands, Germany, and Denmark as shown). External systems are modelled at national and sub-national resolution and provide price-responsive import and export opportunities, subject to interconnector limits, the assumed generation mix, and input costs.

The model is solved at hourly resolution over a full year. Hourly zonal demand and VRE output profiles are constructed using historical weather-based generation data, preserving the underlying temporal correlation between wind, solar, and demand across zones and countries. All simulations, therefore, respect the joint distribution of demand and renewable output rather than relying on representative hours or stylised profiles. Full details of data construction and coverage are provided in Appendix 1.

3.2.2 Generation technologies and operational constraints

The generation mix includes variable renewables (onshore wind, offshore wind, and solar PV), dispatchable thermal plant, nuclear generation, and storage. Nuclear and waste-to-energy units are treated as must-run within technical limits, reflecting their cost[4] and system stability (inertial) characteristics. Dispatchable fossil generation is dispatched subject to capacity limits and variable operating costs.

System-wide feasibility constraints are imposed: instantaneous VRE output is capped at a fixed share (90%) of demand plus exports and storage charging, representing limits on non-synchronous penetration (SNSP). When this constraint binds, additional VRE output must be curtailed, irrespective of transmission availability. These constraints interact with internal

[4] Such as the increased cost of reducing then increasing output that encourages negative bidding for decreasing output.

transmission limits and play an important role in shaping the timing and location of curtailment.

Transmission losses are not modelled explicitly. Instead, zonal transmission marginal cost adders are applied to reflect the increasing marginal losses associated with longer power transfers.[5] These adders stabilise curtailment ordering across zones when multiple feasible curtailment patterns exist with identical short-run costs. They do not affect outcomes when internal constraints do not bind, nor do they affect the measurement of total or marginal curtailment.

3.2.3 Identification of marginal curtailment

Average curtailment for each technology and zone is computed as the ratio of total curtailed energy to total potential output over the simulation horizon as in 3.1. Marginal curtailment is identified through controlled, zone-specific perturbations to VRE capacity. For each technology *i* and zone *z*, installed capacity is increased to give an increase in average potential output of 200 MW on a GB-wide hourly basis. This increment is applied one zone at a time, holding all other capacities and system assumptions fixed. The resulting change in total curtailment, aggregated over all zones and hours, is used to compute marginal curtailment as defined in Section 3.1. The size of the increment reflects a trade-off between numerical stability and marginality. The perturbations are small relative to installed capacity but large enough to avoid rounding artefacts in the optimisation. Sensitivity tests confirm that marginal curtailment estimates are locally linear over a wide range of increment sizes, consistent with earlier results reported in Newbery and Chyong (2025).

3.2.4 Scenario design

The analysis is structured around a set of scenarios designed to isolate the mechanisms identified in Section 3.1. The baseline reflects the 2030 assumptions of the Electricity System Operator's *Future Energy Scenario Hydrogen Evolution* (which has a larger share of conventional generation), including projected VRE capacities, demand, interconnector availability, storage and nuclear commissioning schedules. Against this baseline, three classes of experiments are conducted (Table 2):

1. Internal transmission reinforcement, comparing curtailment outcomes under 2023 and 2030 internal transfer capacities while holding generation fixed.
2. Zone-by-zone VRE expansion, used to identify marginal curtailment and derive zone- and technology-specific LMCoEs.
3. Higher European VRE penetration, reflecting more ambitious National Energy and Climate Plan outcomes and their implications for GB export opportunities.

Each experiment modifies a single dimension of the baseline in a controlled manner, allowing changes in curtailment and costs to be attributed unambiguously to the mechanism under

[5] In GB, transmission losses are used in the dispatch merit order for balancing and charged to consumers.

consideration. We commend this as a way of providing useful policy-relevant information when running large and often opaque dispatch models.

Table 2: Case design and model output metrics

Experiment	Constraints	VRE capacity change	External assumption	Output metrics
Boundary reinforcement	Compare 2023 vs 2030 transfer limits	None	FES HE	Curtailment differences by zone & tech; total reduction
Zone-by-zone VRE increments	2030 transfer limits	One-zone increment at a time (+200 MWh/h GB avg by tech)	FES HE	Δcurtailment, *mc*, *ac*, and *PCF/MCF* multipliers 1/(1-*mc*)
High EU VRE	2030 transfer limits	None	Higher EU VRE penetration (NECP)	Curtailment by zone; % increase; change in GB net exports

GB provides a particularly suitable setting for analysing marginal curtailment under internal transmission constraints. It combines high and rapidly growing VRE penetration, pronounced spatial variation in renewable resource quality, persistent internal congestion, and substantial interconnection with neighbouring systems. These features are not unique to GB but are increasingly common in decarbonising power systems. The results should, therefore, be interpreted as illustrating general mechanisms rather than as producing system-specific forecasts.

4. Modelling results

Table 3 reports key results for the baseline 2030 FES HE with internal constraints and compares them with the benchmark copper plate case taken from Newbery and Chyong (2025). With zonal constraints, total VRE curtailment is 10,426 GWh, 19% higher than under copper plate (8,771 GWh). Curtailment is highly concentrated: Z1 and Z2 together contribute 86% of the total. Z1 is curtailed 1,852 hours, and Z2 is curtailed 948 hours. Z1 is always curtailed when Z2 is curtailed, underscoring the dominance of the B6 boundary at the Scottish border (Figure 1).

Technology shares differ across zones: Z4 and Z6 have the highest shares of offshore wind, Z5 and Z7 of PV, and Z1 and Z2 of onshore wind, so pro-rata curtailment at the zonal level amplifies technology-specific effects relative to national pro-rata curtailment.

External trade impacts are modest: the average absolute hourly difference in exports between zonal pricing and copper plate is 37 MW (standard deviation 166 MW), and total GB external exports fall by about 1%. Exports do little to relieve internal constraints because Scottish zones Z1 can only export to Z2 and Z2 can export only modest volumes to the SEM, as the larger Norway link is in the English zone Z3.

Table 3: Zonal results in 2030 GB FES HE scenario

Baseline	Z1	Z2	Z3	Z4	Z5	Z6	Z7	Total	Copper Plate
Capacity (MW)									
OFF	4,356	3,516	2,890	11,785	5,824	11,708	3,399	43,476	43,476
ON	6,930	9,672	908	2,071	2,698	271	530	23,081	23,081
PV	743	628	1,530	3,730	14,598	1,098	5,318	27,644	27,644
VRE	12,028	13,817	5,328	17,586	23,119	13,076	9,246	94,201	94,201
Transmission marginal costs (€/MWh)	€0.50	€0.40	€0.30	€0.20	€0.00	€0.10	€0.10		
Potential output (GWh)									
OFF	18,785	15,202	13,034	55,148	27,582	54,483	14,619	198,854	198,854
ON	16,996	23,653	2,285	5,159	6,865	687	1,291	56,935	56,935
PV	575	511	1,378	3,234	13,827	1,108	5,565	26,199	26,199
VRE	36,356	39,366	16,698	63,540	48,274	56,278	21,475	281,988	281,988
Curtailment (GWh)									
OFF	2,559	1,264	190	456	306	56	80	4,910	6,075
ON	2,784	2,308	39	50	90	1	8	5,280	2,088
PV	43	33	16	22	102	1	20	236	608
VRE	5,386	3,604	245	527	497	58	108	10,426	8,771
Average curtailment (% of potential output)									
OFF	13.6%	8.3%	1.5%	0.8%	1.1%	0.1%	0.5%	2.5%	1.6%
ON	16.4%	9.8%	1.7%	1.0%	1.3%	0.1%	0.7%	9.3%	1.0%
PV	7.5%	6.4%		0.7%	0.7%	0.1%	0.4%	0.9%	0.3%
VRE	14.8%	9.2%	1.5%	0.8%	1.0%	0.1%	0.5%	3.7%	1.1%
Zonal average trade (MW)	3,016	2,394	498	3,195	-15,721	6,823	-205		

Notes: Copper plate results from Newbery and Chyong (2025); OFF: offshore wind, ON: onshore wind.

4.1 Boundary reinforcement: effect of internal transfer limits on curtailment

Holding 2030 VRE capacities fixed, Table 4 compares curtailment under 2023 internal boundary transfer capacities with curtailment under the higher 2030 transfer capacities. Aggregate VRE curtailment falls from 46,326 GWh to 10,426 GWh, a reduction of 35,900 GWh (77%). Most of this reduction occurs in Z6, where curtailment falls from 30,975 GWh to 58 GWh.

Table 4 also shows that the reduction in curtailment is not uniform across zones. Curtailment is lower in Scottish Z1 and Z2 under 2030 transfer capacities, while curtailment is higher south of the border in Z3-Z5. This pattern is consistent with curtailment being shaped by binding internal constraints and the rerouting of surplus generation across zones when transfer capability is expanded, as set out in the stylised framework in Section 3.1.

Table 4: VRE Curtailment: 2030 vs 2023 transmission capacity

		Z1	Z2	Z3	Z4	Z5	Z6	Z7	Total
2030 Transmission Capacity	GWh	5,386	3,604	245	527	497	58	108	10,426
2023 Transmission Capacity	GWh	9,720	4,910	162	280	226	30,975	54	46,326
difference	GWh	4,334	1,306	-83	-247	-272	30,917	-54	35,900

4.2 Zone-by-zone VRE increments: marginal curtailment

The next set of experiments increases one VRE technology in one zone at a time, holding all other capacities and assumptions fixed, to identify marginal curtailment, *mc*, as defined in Section 3.1. Table 5 reports the incremental potential output associated with each zonal perturbation ("delta potential output"), the corresponding increase in total curtailment relative to the baseline ("delta curtailment"), and the implied marginal curtailment rate *mc*.

To illustrate the interpretation, increasing offshore wind in Z1 yields an incremental potential output of 166 GWh and increases total curtailment by 57 GWh relative to the baseline, giving *mc* = 34% (= 57/166). The lower panel reports the associated scaling factors 1/(1-*mc*), consistent with equations (2)-(4) in Section 3.1.

Table 5 shows substantial variation in *mc* across zones and technologies. For onshore wind, *mc* is 48% in Z1 and 47% in Z2, compared with values between 0% and 24% in Z3-Z7. For offshore wind, *mc* is 34% in Z1 and 36% in Z2, compared with 16-17% in Z3-Z7. For solar PV, *mc* ranges from 10% to 26% across zones, with 26% in Z1 and Z2 and 10-17% in Z3-Z7. These results imply that the proportional cost uplift captured by 1/(1-*mc*) is markedly larger in Z1-Z2 for wind technologies than in the other zones.

Table 5 applies common zonal potential capacity factor assumptions for wind technologies, reflecting the interpretation that within-zone site selection leads developers to locate in the best wind resource areas within each zone. For solar PV, zonal-average potential capacity factors are retained, and the final line of Table 6 reports the corresponding scaled PV factor, as indicated in the table notes.

Appendix 2 (Table A7) reports the distribution of curtailment changes by zone associated with each increment, showing that an increment in one zone can change curtailment in other zones.

Table 5: Marginal contributions of additional VRE capacity, zone by zone

		Z1	Z2	Z3	Z4	Z5	Z6	Z7	total
delta potential output, GWh	OFF	166	134	115	486	243	480	129	1753
	ON	523	728	70	159	211	21	40	1752
	PV	38	34	92	216	922	74	371	1747
delta curtailment, GWh	OFF	57	48	20	84	39	80	22	350
	ON	249	339	15	39	48	0	6	694
	PV	10	9	11	22	115	13	38	218
***mc p.c. of* potential output**	OFF	34%	36%	17%	17%	16%	17%	17%	20%
	ON	48%	47%	21%	24%	23%	0%	14%	40%
	PV	26%	26%	12%	10%	12%	17%	10%	12%
***ac* p.c. pot. output**	PV	8.9%	9.3%	10.3%	9.9%	10.8%	11.5%	12.0%	11%
1/(1-*mc*)	OFF	1.52	1.56	1.21	1.21	1.19	1.20	1.20	1.25
	ON	1.91	1.87	1.27	1.32	1.29	1.00	1.16	1.66
	PV	1.35	1.36	1.14	1.11	1.14	1.21	1.11	1.14
scaled for PV CF*	PV	1.67	1.61	1.22	1.24	1.16	1.15	1.03	1.14

Notes: OFF: offshore wind, ON: onshore wind.

** Scaled for the average PV zonal capacity factors to give the relevant PCF/MCF.*

4.3 Higher European VRE penetration: sensitivity to export opportunities

The final experiment tests how GB curtailment changes when higher wind and solar deployment in Europe reduces Britain's ability to export surplus VRE output. Table 6 reports curtailment by zone under the higher European VRE assumption and compares it with the baseline. Total VRE curtailment increases from 10,426 GWh to 16,904 GWh, an increase of 6,478 GWh (62%). Net exports fall from 35 TWh to 18 TWh.

The proportional increase in curtailment differs across zones. Table 6 shows increases of 37% in Z1 and 80% in Z2, compared with increases above 100% in Z3-Z7. In the baseline, the central and southern zones are also those with larger interconnector access, as set out in Section 3.2.1 and Table 1, and the result is consistent with the mechanism that export headroom influences the ability to absorb surplus VRE output.

Table 6: Impact of higher EU VRE penetration

	Z1	Z2	Z3	Z4	Z5	Z6	Z7	Total
high EU VRE curtailment, GWh	7,365	6,491	527	1,061	1,106	122	233	16,904
baseline curtailment, GWh	5,386	3,604	245	527	497	58	108	10,426
Increase,	1,980	2,887	281	534	609	64	124	6,478
p.c. increase	37%	80%	115%	101%	122%	111%	114%	62%

5. Cost Implications

Curtailment reduces the share of potential output ultimately delivered to the system, thereby raising the cost per delivered MWh. Section 3.1 distinguished between two delivered-cost concepts relevant to investment appraisal. The levelised average cost of delivered electricity (LACoE) adjusts the underlying levelised cost of electricity (LCoE) for average curtailment through the delivered average capacity factor. As noted earlier, this is relevant where developers pay shared deep connection charges and accept curtailment without compensation.

In contrast, the levelised marginal cost of delivered electricity (LMCoE) applies the same adjustment using marginal curtailment and the delivered marginal capacity factor. The distinction is economically important because marginal curtailment can exceed average curtailment by a wide margin in specific locations, implying that the cost penalty faced by incremental investment may be substantially larger than average outcomes suggest.

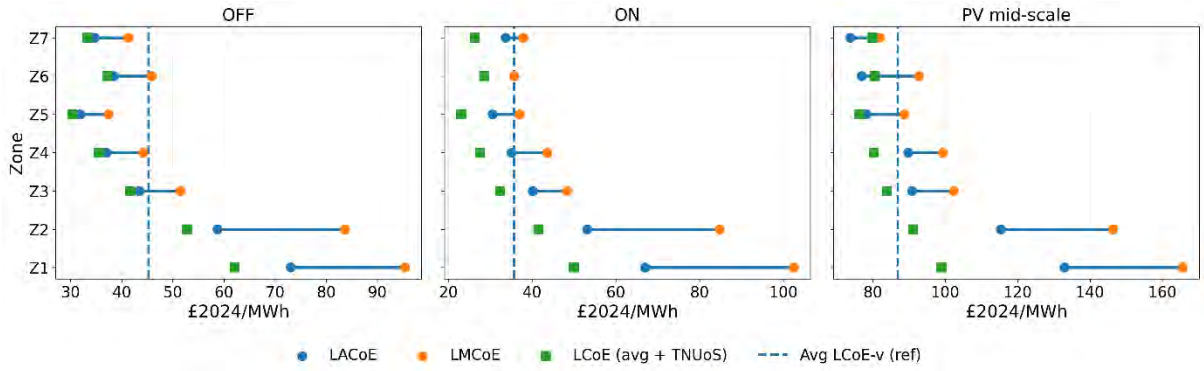

Figure 2: Location-specific divergence between average and marginal delivered costs for variable renewables.
Notes: The figure highlights large spatial differences in marginal delivered electricity costs that are not captured by average curtailment or headline LCoE measures. These differences arise from the interaction between marginal curtailment and internal transmission constraints, and are most pronounced in zones where curtailment is already high. Values are expressed in £2024/MWh and reflect construction costs for 2030 as in BEIS (2023).

Figure 2 summarises these relationships by zone and technology. For each zone, the figure reports three related objects: the zonal benchmark LCoE net of variable operating costs and adjusted for network charges (see Table A. 3, Appendix 1); the corresponding LACoE based on average curtailment (Table A9, Appendix 2); and the LMCoE implied by marginal curtailment (Table A10, Appendix 2). The figure, therefore, separates location-specific cost differences arising solely from network charges from those that emerge endogenously through curtailment, and shows how marginal investment costs diverge from average delivered costs in constrained parts of the system.

Two patterns stand out. First, there is a pronounced spatial gradient in delivered costs for wind technologies. In the northern (Scottish) zones (Z1 and Z2), where marginal curtailment rates are highest, LMCoE substantially exceeds both the zonal LCoE benchmark and the corresponding LACoE. For offshore wind, LMCoE exceeds £90/MWh in Z1 and remains above £80/MWh in Z2, while falling below £50/MWh in the southern and central zones. A similar pattern is observed for onshore wind, with LMCoE above £100/MWh in Z1 and below £40/MWh in the least constrained zones. These differences are an order of magnitude larger than the underlying variation in headline LCoE assumptions and reflect the amplification effect of marginal curtailment rather than differences in technology costs per se.

Second, the divergence between LACoE and LMCoE is itself strongly location-specific. In zones with low marginal curtailment, average and marginal delivered costs remain close, indicating that average curtailment provides a reasonable approximation to the cost impact of

incremental investment. However, in zones with high marginal curtailment, LACoE understates the cost faced by additional capacity by a wide margin. This is most evident in Z1 and Z2, where the gap between LACoE and LMCoE is large across wind technologies, reflecting the fact that incremental output is curtailed disproportionately relative to average output.

Solar PV exhibits the same qualitative pattern, though with a less extreme gradient. Marginal delivered costs are again highest in Z1 and Z2 and fall sharply in zones with lower marginal curtailment. For PV mid-scale, the absolute level of LMCoE is higher across all zones due to the higher underlying LCoE assumption. Still, the spatial structure remains governed by curtailment rather than by technology costs alone.

These results arise mechanically from the non-linear scaling relationship between delivered costs and marginal curtailment derived in Section 3.1. Where marginal curtailment is already elevated, even modest further increases translate into disproportionately large increases in the cost per delivered MWh. The delivered-cost gradients observed in Figure 2, therefore, reflect the interaction between internal transmission constraints and incremental investment, rather than differences in resource quality or technology cost assumptions across zones.

Full numerical results underlying Figure 2, including the construction of LACoE and LMCoE from zonal curtailment outcomes and cost assumptions, are reported in Appendices 1 and 2. The sensitivity results under higher European VRE penetration further reinforce this conclusion: reductions in export headroom raise marginal curtailment most sharply in already-constrained zones, leading to additional increases in marginal delivered costs that are concentrated spatially rather than evenly spread across the system.

6. Discussion and policy implications

This article quantifies how binding internal transmission constraints raise marginal curtailment and, through that channel, create significant spatial differences in the marginal cost of delivered electricity from wind and solar investment. The underlying mechanism is that when congestion and system stability limits (SNSP) bind in a limited set of hours, incremental output is disproportionately curtailed relative to the existing fleet. Because delivered costs scale non-linearly with marginal curtailment, moderate differences in *mc* imply large differences in the long-run marginal cost of investment, LMCoE.

The transmission reinforcement experiment highlights the first-order role of internal transfer capacity. Holding the 2030 generation portfolio fixed, increasing internal transfer limits from 2023 to 2030 levels reduces total curtailment from 46,326 GWh to 10,426 GWh, a reduction of 35,900 GWh (77%). The reduction is concentrated in Z6, where curtailment falls from 30,975 GWh to 58 GWh, while curtailment increases in Z3-Z5. Reinforcement can, therefore, sharply reduce curtailment in particular constrained areas, but it also reroutes surplus flows and changes where curtailment is ultimately absorbed.

The zone-by-zone increment experiments show that marginal curtailment varies sharply across locations. For onshore wind, *mc* is 48% in Z1 and 47% in Z2, compared with 0-24% in Z3-Z7. For offshore wind, *mc* is 34% in Z1 and 36% in Z2, compared with 16-17% in Z3-Z7.

These differences imply large gradients in marginal delivered costs. Offshore wind LMCoE is £95.36/MWh in Z1 and £83.64/MWh in Z2, compared with £37.39/MWh in Z5 and £41.32-£51.48/MWh in Z3-Z7. For onshore wind, LMCoE is £102.46/MWh in Z1 and £84.74/MWh in Z2, compared with £35.73/MWh in Z6 and £37.02-£48.29/MWh in Z3-Z7. By comparison, the corresponding LACoE values are materially lower in the high-curtailment zones, reflecting the fact that average curtailment does not capture the conditions faced by incremental investment where congestion binds.

The high-EU-VRE sensitivity indicates that GB curtailment also depends on external conditions that determine export headroom. With higher European wind and solar deployment, total GB curtailment increases from 10,426 GWh to 16,904 GWh (62%), while net exports fall from 35 TWh to 18 TWh. Curtailment increases by more than 100% in Z3-Z7, compared with 37% in Z1 and 80% in Z2. This pattern is consistent with the distribution of interconnectors access across zones and with correlated surplus conditions as neighbouring systems decarbonise.

These results bear directly on how REMA has been framed: greater spatial granularity in wholesale prices versus retaining a national, uniform price, combined with stronger locational signals delivered through other channels. The modelling evidence points to persistent, location-specific differences in the marginal cost of delivered renewable output, driven primarily by congestion-induced marginal curtailment rather than by assumed technology costs. Under a national wholesale price, the central issue is whether the investment environment makes these location-specific marginal delivered-cost consequences visible to developers and financiers. If not, decentralised investment will tend to concentrate in high-resource areas even when marginal curtailment erodes delivered value. For wind, the implied wedge between Z1 (north) and the least-constrained zones is of the order of £50-£70/MWh in LMCoE terms, which is too large to treat as a minor adjustment.

A practical test for Reformed National Pricing in GB (and changes in transmission charges) is, therefore, whether it reduces the gap between private incentives and the marginal delivered costs implied by *mc* and LMCoE. Instruments that sharpen locational signals without moving to nodal prices are likely to matter most where *mc* is highest and where the cost amplification is steepest.

The results are also directly relevant to renewable support, because contract design determines how curtailment risk is allocated and whether investors face incentives aligned with location-specific marginal delivered costs. If support arrangements treat curtailed output as close to equivalent to delivered output, then projects in high-*mc* zones can appear privately attractive even when the cost of delivered energy from additional capacity is high. Conversely, where contracts expose projects to predictable curtailment risk, or where procurement places more weight on delivered energy, incentives move closer to the system objective of procuring low-carbon electricity at least cost.

Three design implications follow.

First, incremental procurement value should be judged using marginal rather than average curtailment. The LMCoE gradients are driven by *mc*, not by *ac*. When *mc* is high, appraisal

based on average curtailment systematically underestimates the cost of delivered output from additional capacity.

Second, locational differentiation can be introduced within a national CfD framework. This does not require nodal prices. It can be implemented through transparent zone- and technology-specific adjustment factors derived from *mc* (or equivalently from LMCoE) when comparing bids, and/or through differentiated procurement volumes or capacity caps in persistently constrained areas.

Third, where congestion is expected to persist, support can be aligned more closely with delivered output while preserving bankability. Network expansion lead times imply that congestion will remain binding for a period even under accelerated reinforcement. Contract structures that tighten the link between remuneration and delivered energy reduce incentives to concentrate new capacity behind already-constrained boundaries. The case is strongest for wind in northern zones (Z1-Z2), where *mc* approaches one-half for onshore wind and exceeds one-third for offshore wind, implying significant marginal delivered-cost uplifts. For example, an option is to offer CfDs that pay on delivered (uncurtailed) output only, but for a specified number of full operating hours (e.g., 40,000 MWh/MW capacity), rather than paying on offers for a fixed number of years (Newbery, 2023).s

Here, we do not attempt a welfare evaluation of specific CfD, transmission access, and charging reforms. The contribution of this article is narrower: it quantifies marginal curtailment and the implied location-specific marginal delivered costs, which can be used to calibrate locational adjustments within support mechanisms in a way that is consistent with the system costs implied by congestion and curtailment.

Beyond CfDs, a small set of complementary tools follows from the mechanisms identified in this research.

First, connection and access arrangements. Distinguishing between firm and non-firm access, and making curtailment risk explicit in connection terms, provides a direct way to translate high marginal curtailment into a private investment signal. For example, developers could be offered a non-firm connection (last in, first off without compensation) for a number of years until export capacity is adequately increased. The aim is not to eliminate curtailment but to avoid systematically adding capacity in locations where incremental output is predictably curtailed.

Second, strategic spatial planning informed by marginal metrics. Publishing zone- and technology-specific indicators of marginal curtailment and implied LMCoE would provide an operational signal for investors and planners. This is particularly relevant under a national price, where locational incentives rely on a combination of charges, planning, and connection rules rather than on granular wholesale locational marginal prices.

Third, network reinforcement prioritised by curtailment elasticities. The reinforcement experiment modelled here shows that increasing transfer limits can materially reduce curtailment, while also redistributing it across zones. A natural implication is to prioritise

reinforcement where additional transfer capability most reduces system-wide marginal curtailment, rather than relying solely on average curtailment levels.

Finally, the high-EU-VRE case indicates that export headroom is unlikely to remain a stable outlet for surplus generation as neighbouring systems deploy wind and solar in correlated hours. This strengthens the case for domestic instruments that steer investment and flexibility to locations where they reduce marginal curtailment.

7. Conclusions and limitations

This article shows that internal transmission constraints can generate significant divergences between average and marginal curtailment and, as a result, substantial spatial differences in the marginal cost of delivered electricity from incremental renewable investment. In the 2030 GB system configuration examined here, marginal curtailment for additional onshore wind is close to one-half in the northern (Scottish) zones (Z1-Z2), while being below one-quarter elsewhere. The implied wind LMCoE estimates differ by tens of pounds per MWh across zones. The results also indicate that curtailment outcomes depend on export headroom, which weakens as neighbouring systems deploy wind and solar in correlated hours. The economic implication is that incremental investment appraisal in constrained systems should be based on marginal curtailment and should be treated as location-specific when congestion persists. This also applies to evaluating interconnector investments.

Several limitations qualify the interpretation. The UCED model captures the main feasibility constraints shaping dispatch and curtailment. However, it does not represent the full range of ancillary service and reserve requirements that may bind at high VRE penetration. Curtailment allocation across technologies within zones and across zones can also depend on modelling conventions when avoidable costs are similar. The marginal curtailment estimates are local to the baseline configuration used here; as network capacity, generation portfolios, and neighbouring-system conditions evolve, *mc* and LMCoE will change. The results are therefore best read as evidence of how congestion reshapes the economics of incremental renewable deployment in a system with binding internal constraints, and as empirical inputs for strengthening locational signals within a national, uniform pricing framework.

References

AFRY Management Consulting (2025a). *Enhanced National Electricity Market Designs for Great Britain.* Report prepared for industry stakeholders, February 2025. https://afry.com/en/enhanced-national-electricity-market-designs-great-britain

AFRY Management Consulting (2025b). *Sensitivity Analysis on the Modelled Benefits of Zonal Electricity Markets in Great Britain.* Report prepared for industry stakeholders, May 2025. https://afry.com/en/sensitivity-analysis-modelled-benefits-zonal-electricity-markets-in-great-britain

Ambrosius, M., Grimm, V., Kleinert, T., Liers, F., Schmidt, M., & Zöttl, G. (2020). Endogenous price zones and investment incentives in electricity markets: An application of multilevel optimisation with graph partitioning. *Energy Economics*, *92*, 104879. https://doi.org/10.1016/j.eneco.2020.104879

Aravena, I., & Papavasiliou, A. (2016). Renewable energy integration in zonal markets. *IEEE Transactions on Power Systems*, *32*(2), 1334-1349. https://ieeexplore.ieee.org/document/7501844

Aurora Energy Research (2023). *Locational Marginal Pricing in Great Britain.* September 2023. https://auroraer.com/wp-content/uploads/2023/09/Locational-Marginal-Pricing-GB-Aurora-Public-Report.pdf

BEIS, 2020. *Electricity Generation Costs (2020)*, https://www.gov.uk/government/publications/beis-electricity-generation-costs-2020

BEIS, 2023. *Electricity Generation Costs (2023)*, October https://www.gov.uk/government/publications/electricity-generation-costs-2023

Bichler, Martin and Dobos, Teodora and Knoerr, Johannes, Zonal vs. Nodal Pricing: An Analysis of Different Pricing Rules in the German Day-Ahead Market. Available at SSRN: https://ssrn.com/abstract=5204814 or http://dx.doi.org/10.2139/ssrn.5204814

Chyong, C., Pollitt, M., & Cruise, R. (2019). Can wholesale electricity prices support "subsidy-free" generation investment in Europe? Available at: https://www.jstor.org/stable/resrep30343?seq=1

Chyong, C. K., & Newbery, D. (2022). A unit commitment and economic dispatch model of the GB electricity market-Formulation and application to hydro pumped storage. Energy Policy, 170, 113213.

Dagoumas, A. S., & N.E. Koltsaklis. 2019. "Review of models for integrating renewable energy in the generation expansion planning**."** *Applied Energy*, 242**,** 1573-1587**.** https://doi.org/10.1016/j.apenergy.2019.03.194

DESNZ, 2024a. *Review of Electricity Market Arrangements Second Consultation* at https://assets.publishing.service.gov.uk/media/65ef6694133c220011cd37cd/review-electricity-market-arrangements-second-consultation-document.pdf

DESNZ, 2024b. *Review of Electricity Market Arrangements Options Assessment* at https://assets.publishing.service.gov.uk/media/65eb48f362ff48ff7487b30a/rema-options-assessment.pdf

DESNZ, 2025a. *Energy Trends: UK Renewables*, at https://www.gov.uk/government/statistics/energy-trends-section-6-renewables

DESNZ, 2025b. *Review of electricity market arrangements (REMA): Summer update, 2025* at https://www.gov.uk/government/publications/review-of-electricity-market-arrangements-rema-summer-update-2025/review-of-electricity-market-arrangements-rema-summer-update-2025-accessible-webpage

Dobos, T., Bichler, M., & Knörr, J. (2025). Challenges in finding stable price zones in European electricity markets: Aiming to square the circle? *Applied Energy*, *382*, 125315. https://arxiv.org/abs/2404.06489

Eicke, A., & Schittekatte, T. (2022). Fighting the wrong battle? A critical assessment of arguments against nodal electricity prices in the European debate. *Energy Policy*, *170*, 113220. https://ssrn.com/abstract=4033908

ENTSO-E, 2022. Report on the Locational Marginal Pricing Study of the Bidding Zone Review Process, at https://eepublicdownloads.blob.core.windows.net/public-cdn-container/clean-documents/Publications/Market%20Committee%20publications/ENTSO-E%20LMP%20Report_publication.pdf

ENTSO-E, 2025. *Bidding Zone Review of the 2025 Target Year.* At https://www.entsoe.eu/network_codes/bzr/#Downloads_of_the_Bidding_Zone_Review_(BZR)_Report_for_the_target_year_2025

EU, 2024. Regulation (EU) 2024/1747 of the European Parliament and of the Council of 13 June 2024 amending Regulations (EU) 2019/942 and (EU) 2019/943 as regards improving the Union's electricity market design (Text with EEA relevance) PE/1/2024/REV/1at https://eur-lex.europa.eu/eli/reg/2024/1747/oj/eng

Frontier Economics & LCP Delta, 2024. *Zonal Pricing in Great Britain: Assessing the Impacts on support payments.* Commissioned report for SSE, October 2024.

FTI Consulting, 2023. *Assessment of locational wholesale electricity market design options in GB*, at https://www.ofgem.gov.uk/sites/default/files/2023-10/FINAL%20FTI%20Assessment%20of%20locational%20wholesale%20electricity%20market%20design%20options%20-%2027%20Oct%202023%205.pdf

FTI Consulting, 2025. Impact of a Potential Zonal Market Design in Great Britain: *Quantitative Assessment of GB Welfare Impacts.* Report for Octopus Energy, February 2025. https://octopus.energy/press/octopus-energy-fti-report-zonal-pricing/

Green, R. (2007). Nodal pricing of electricity: how much does it cost to get it wrong? *Journal of Regulatory Economics*, **31**(2), 125-149. https://doi.org/10.1007/s11149-006-9019-3

HM Government, 2022. *Review of electricity market arrangements (REMA)*, published July 2022. https://www.gov.uk/government/collections/review-of-electricity-market-arrangements-rema#rema-consultations

Katzen, M., & Leslie, G. W. (2024). Siting and operating incentives in electrical networks: A study of mispricing in zonal markets. *International Journal of Industrial Organization*, *94*, 103069. https://doi.org/10.1016/j.ijindorg.2024.103069

Kenis, M., Dvorkin, V., Schittekatte, T., Bruninx, K., Delarue, E., & Botterud, A. (2024). Evaluating Offshore Electricity Market Design Considering Endogenous Infrastructure Investments: Zonal or Nodal? *IEEE Transactions on Energy Markets, Policy and Regulation*. https://ieeexplore.ieee.org/document/10530165

Koltsaklis, N. E., & A.S. Dagoumas. 2018. State-of-the-art generation expansion planning: A review. *Applied Energy*, 230, 563-589. https://doi.org/10.1016/j.apenergy.2018.08.087

Kröger. M. and D. Newbery, 2024. Renewable electricity contracts: lessons from European experience, *Papales de Energiá*, 24 at https://www.funcas.es/revista/papeles-de-energia-24/

LCP Delta (2024). *Zonal Pricing in Great Britain: Assessing the impacts of the 'Beyond 2030' Network Plans.* Commissioned report for SSE, October 2024. https://www.sse.com/media/x3ehjdpg/lcp-d-sse-impacts-of-beyond-2030-network-plans-on-zonal-pricing-october-2024.pdf

Li, C., C.K. Chyong, D. Reiner & F. Roques. 2024. Taking a Portfolio approach to wind and solar deployment: The case of the National Electricity Market in Australia. *Applied Energy*, 369. DOI: https://doi.org/10.1016/j.apenergy.2024.123427

Lindberg, M. B. (2022). The power of power markets: Zonal market designs in advancing energy transitions. *Environmental Innovation and Societal Transitions*, *45*, 132-153. https://doi.org/10.1016/j.eist.2022.08.004

Loiacono, L., Rizzo, L., & Stagnaro, C. (2025). Impact of bidding zone re-configurations on electricity prices: Evidence from Sweden. *Energy Economics*, *141*, 108106. https://doi.org/10.1016/j.eneco.2024.108106

Lundin, E. (2022). Geographic price granularity and investments in wind power: Evidence from a Swedish electricity market splitting reform. *Energy Economics*, *113*, 106208. https://doi.org/10.1016/j.eneco.2022.106208

Neuhoff, K., Barquin, J., Bialek, J. W., Boyd, R., Dent, C. J., Echavarren, F., ... & Weigt, H. (2013). Renewable electric energy integration: Quantifying the value of design of markets for international transmission capacity. *Energy Economics*, *40*, 760-772. https://doi.org/10.1016/j.eneco.2013.09.004

Newbery, D. 2021. National Energy and Climate Plans for the island of Ireland: wind curtailment, interconnectors and storage. *Energy Policy* 158, 112513, 1-11. https://doi.org/10.1016/j.enpol.2021.112513

Newbery, D., 2023. Designing efficient Renewable Electricity Support Schemes, *The Energy Journal*, Vol. 44(3), 1-22., https://doi.org/10.5547/01956574.44.3.dnew

Newbery, D. 2025. Implications of Renewable Electricity Curtailment for Delivered Costs, *Energy Economics*, May. https://doi.org/10.1016/j.eneco.2025.108472

Newbery, D. and Chyong, C-K. 2025. Marginal curtailment and the efficient cost of clean power. EPRG WP2505. https://www.jbs.cam.ac.uk/wp-content/uploads/2025/05/eprg-wp2505.pdf

Newbery, D. and D. Biggar. 2024. Marginal curtailment of wind and solar PV: transmission constraints, pricing and access regimes for efficient investment. *Energy Policy* 191, 114206. https://doi.org/10.1016/j.enpol.2024.114206

Oree, V., S. Hassen & P. Fleming. 2017. Generation expansion planning optimisation with renewable energy integration: A review. *Renewable and Sustainable Energy Reviews*, 69, 790-803. https://doi.org/10.1016/j.rser.2016.11.120

Savelli, I., Hardy, J., Hepburn, C., & Morstyn, T. (2022). Putting wind and solar in their place: Internalising congestion and other system-wide costs with enhanced contracts for difference in Great Britain. *Energy Economics*, *113*, 106218. https://doi.org/10.1016/j.eneco.2022.106218

Simshauser, P. and D. Newbery, 2024. Non-firm vs priority access: On the long run average and marginal costs of renewables in Australia, *Energy Economics*, 136, 107671. https://doi.org/10.1016/j.eneco.2024.107671

Triolo, R. C., & Wolak, F. A. (2022). Quantifying the benefits of a nodal market design in the Texas electricity market. *Energy Economics*, *112*, 106154. https://doi.org/10.1016/j.eneco.2022.106154

Wolak, F. A. (2011). Measuring the benefits of greater spatial granularity in short-term pricing in wholesale electricity markets. *American Economic Review*, *101*(3), 247-252. https://doi.org/10.1257/aer.101.3.247

Zarnikau, J., Woo, C. K., & Baldick, R. (2014). Did the introduction of a nodal market structure impact wholesale electricity prices in the Texas (ERCOT) market? *Journal of Regulatory Economics*, *45*, 194-208. https://doi.org/10.1007/s11149-013-9240-9

Appendix 1: Data Sources for the UCED Model

This appendix lists data sources and their processing and transformation calibrated to projections from the *Future Energy Scenarios Hydrogen Evolution* (*FES HE*, ESO 2024a,b) and ENTSO-E *TYNDP 2022*. It also describes GB's interconnector capacity and storage capacity in 2023.

Demand

The model considers 19 European national electricity markets (Table A.1), divided into 28 zones to explicitly account for key sub-national transmission constraints in GB (7 zones), Denmark (2 zones), and Norway (3 Zones). Annual demand (in TWh) is for *Hydrogen Evolution* (ESO, 2024b).[6] Annual projections were multiplied by hourly load profiles to give hourly load time series for the dispatch model. The hourly profiles were taken from PECD (2021). The 1998 climate year was chosen to represent a normal year (Ah-Voun et al., 2024) to preserve spatial correlation between GB and European markets, as well as hourly wind and solar capacity factors (from ***TYNDP 2022***, Appendix VI: Demand). These hourly load profiles vary by scenario and are created bottom-up based on different types of demand (e.g., electric vehicles, heat pumps/electric heating). All inputs will be available at https://github.com/KongChyong

Table A.1 Annual electricity demand (TWh) projection for 2030

Country	Country Code	2030	Country	Country Code	2030
GB1	GB	5.87	Spain	ES	286.63
GB2	GB	15.85	Finland	FI	103.15
GB3	GB	14.57	France	FR	516.22
GB4	GB	56.00	Italy	IT	380.75
GB5	GB	178.05	Luxembourg	LU	9.01
GB6	GB	5.73	Netherlands	NL	180.39
GB7	GB	38.29	Norway	NO	170.26
Austria	AT	84.35	Poland	PL	197.6
Belgium	BE	99.47	Portugal	PT	60.88
Switzerland	CH	71.68	Sweden	SE	168.69
Czech Republic	CZ	80.96	SEM	SEM	52.17
Germany	DE	684.36	Slovenia	SI	16.59
Denmark	DK	54.42			

Generation

Electricity generation in the model includes gas, thermal coal, oil, biomass, low-carbon hydrogen, nuclear, solar PV, wind, and other renewable supplies (RES, such as marine and waste energy). Gross installed capacity was taken from *FES HE* scenario 2030 for GB (tab "ES1") and Europe (tab "ES2"). Table A. 4 reports the total installed generation capacity per country in the model.

Technoeconomic parameters such as ramp rates, minimum up and downtime, start-up and shutdown costs, thermal efficiency, and variable operating and maintenance (non-fuel) costs for dispatchable generation were primarily sourced from ENTSOE's ERAA 2023 Study.[7] All costs and prices used in the model are Euro 2023 prices.

The installed capacities were primarily sourced from the FES HE scenario (ESO, 2024) dataset, with GB-wide solar and wind hourly capacity factors (CFs) obtained from the PECD (2021) for the 1998 climate year. The GB zonal VRE capacity factors were sourced from

[6] GB demand is at tab ES1, EU demand at tab ES2.

[7] The original source for these parameters is the worksheet titled "Thermal Properties" within the Excel file named "ERAA2023 PEMMDB Generation.xlsx", derived from the Pan-European Market Modelling Database.

https://www.renewables.ninja/, selecting representative NUTS-2 regional hourly CFs and adjusting them as explained below to obtain the final CFs, whose zonal averages are given in Table A. 2. For solar technologies, the analysis distinguished between utility-scale and rooftop PV installations. Rooftop solar profiles were adjusted for utility-scale PV using a factor of 1.11, derived from Jacobson and Jadhav (2018), to account for differences in sunlight incidence due to panel tilt and tracking. Weighted averages were then calculated for each zone, incorporating sub-zonal capacities for utility and rooftop solar.

The PECD climate database for Europe treats GB as a single zone. Further, the PECD database is a composite "normal" climate year rather than a specific year, although it is based on 1998 data. Its correlation with the actual Ninja data[8] for GB onshore wind in 1998 is 99%, and that is the year chosen for downloading Ninja data at the NUTS level, disaggregated to hourly resolution. Zonal values were calculated for the one or two NUTS regions with the highest average CFs (see Table A.2) and averaged, on the basis that developers would choose the most favourable locations within zones. Offshore hourly CFs are taken from the nearest onshore NUTS (in some cases, the average of the east and west coast values). For PV, representative zonal longitude and latitude values were used to download suitable Ninja CFs, which were then scaled as for other VREs.

The resulting zonal hourly capacity factors ($CF_{z,h}$) reflect the cross-zonal correlations of weather. A consistent zonal VRE hourly output involves scaling $CF_{z,h}$ to preserve the GB-level zonal aggregate output correlation with the PECD GB data. The first step involved scaling and then flattening the $CF_{z,h}$ to ensure that they remain within the range [0%,100%]. Let $\sum_z CF_{z,h}K_z / Y_h = \theta_h$ be a scaling factor, where Y_h is the PECD hourly output. As this varies between 0.16 and 1.54 for onshore wind, simply scaling by this factor would produce CFs outside the acceptable range. The next adjustment is first, to scale the original $CF_{z,h}$ to revised CFs: $CF^*_{z,h} = 0.5\theta_h + (1- 0.5\theta_h * CF_{z,h})$ and then rescale by a further scaling factor $\varphi_h = \sum_z CF^*_{z,h}K_z / Y_h$, which gives a GB hourly aggregate equal to the PECD value and preserves the cross-zonal correlations. The same approach was followed for offshore wind, except for a few cases in which the resulting $CF_{z,h}$ exceeded 100% and was capped at 100%. It should be recognised that actual windfarms might have quite different CFs even in the same zone. Still, the purpose of the zonal exercise is to capture boundary constraints at any hour, and for that, good correlations within the zone are more important than the actual CFs.

This method fails for PV because the scaling factors can be too high and produce improbable hourly CFs; these were capped at the centred monthly NUTS zonal values, then scaled hourly to be consistent with the PECF GB hourly values, and finally capped at the maximum value of the original zonal CFs. Table A.2 lists the NUTS 2 zones used for onshore wind CFs, while the map shows their locations.[9]

[8] From Renewables.ninja Wind (NUTS-2 hourly data, 1980-2019) - ninja_wind_country_GB_merra-2_nuts-2_corrected - Version: 1.3 - License: https://creativecommons.org/licenses/by-nc/4.0/ - Reference: https://doi.org/10.1016/j.energy.2019.08.060

[9] At https://commons.wikimedia.org/wiki/File:NUTS_2_statistical_regions_of_the_United_Kingdom_2015_map.svg

Table A. 2: GB Zonal wind and solar potential capacity factors (PCF)

Zone	NUTS2	OFF	ON	PV
Z1	M5-6	49.2%	28.0%	8.8%
Z2	M2-3	49.4%	27.9%	9.3%
Z3	C2,D1	51.5%	28.7%	10.3%
Z4	L1,E1	53.4%	28.4%	9.9%
Z5	F3,L1	54.1%	29.0%	10.8%
6	H1	53.1%	28.9%	11.5%
Z7	K2, J2	49.1%	27.8%	11.9%
GB		52.2%	28.2%	10.8%

At present, NESO charges intermittent generators an annual charge in £/kW that varies by location. The charge is made up of a year-round shared element x Average CF + a year-round non-shared element + adjustment tariff. If a transmission-connected generator is directly connected to a substation that is defined as a Main Interconnected Transmission System (MITS) node, it will only need to pay the onshore local substation tariff.[10] The following table starts from the assumed grid and the connection charges already included in the Levelised Cost of Electricity (LcoE) in BEIS (2020, 2023), and adds deviations of the TNUoS zonal charge from the average across all NESO zones (on the assumption that the LcoEs used average figures). Thus, in Z1, the TNUoS charge for offshore wind is £25.34/kWyr, but the average is £8.52/kWyr and this is deducted, resulting in an additional charge of £16.83/kWyr. To add to the LcoE. The results are shown in Table A. 3.

Table A. 3: Levelised costs and TNUoS adders for 2030, £(2024)/MWh

Zone	OFF	ON	PV	PV mid-scale
Z1	£16.83	£14.27	£12.02	£12.02
Z2	£7.51	£5.76	£4.21	£4.21
Z3	-£3.57	-£3.29	-£3.04	-£3.04
Z4	-£9.72	-£8.10	-£6.66	-£6.66
Z5	-£14.92	-£12.61	-£10.58	-£10.58
Z6	-£8.05	-£7.15	-£6.35	-£6.35
ssZ7	-£11.91	-£9.34	-£7.06	-£7.06
LCoE	£46.44	£42.87	£44.06	£86.93
variable cost *v*	£1.19	£7.15	£0.00	£0.00
LCoE-*v*	£45.25	£35.73	£44.06	£86.93

Source: BEIS (2025), uprated to £2024 with the CPI

[10] https://www.neso.energy/document/130271/download

Table A. 4: Electricity generation capacity by fuels in 2030 (MW)

	Biomass	Coal	Gas	Oil	Hydrogen	Other RES	Solar	Wind Onshore	Nuclear	Wind Offshore	Total
Austria	585		1,997	164		293	9,620	8,691			**21,349**
Belgium	668		8,772	150		452	9,590	4,396	2,077	5,805	**31,909**
Czech Republic	410	3,690	856		500		6,080	1,506	3,936		**16,978**
Denmark	2,534		628				5,029	5,479		9,730	**23,401**
Finland	1,600		2,969				3,185	14,326	3,380	7,101	**32,561**
France	2,120		12,486	1,041	500	240	38,769	29,632	60,320	4,964	**150,072**
Germany	12,110		35,604	857	500	2,100	156,298	82,128		28,021	**317,619**
GB1	86		2,309	52		85	743	6,930		4,356	**14,561**
GB2	62		38	52		40	628	9,672		3,516	**14,009**
GB3	366		392	52		299	1,530	908		2,890	**6,437**
GB4	2,248		11,101	52		1,252	3,730	2,071		11,785	**32,240**
GB5	1,111		23,911	52		3,747	14,598	2,698	2,709	5,824	**54,649**
GB6	69		1,234	52		82	1,098	271	1,861	11,708	**16,375**
GB7	285		4,426	52		314	5,318	530		3,399	**14,323**
Island of Ireland (SEM)			7,723	693		103	4,496	8,749		4,344	**26,107**
Italy	4,672		50,222				63,568	16,743		1,940	**137,145**
Netherlands	1,059		15,386				28,084	7,795	485	16,979	**69,788**
Norway	732						2,563	6,369		8,779	**18,444**
Poland	1,535	16,584	8,182				15,597	15,554		10,560	**68,012**
Portugal	700		4,016				13,490	9,751		330	**28,287**
Slovenia	23	539	460				1,768	981	696		**4,467**
Spain	1,100		18,875		200		55,227	41,035	4,104	1,680	**122,221**
Sweden	2,220						4,830	22,459	6,881	1,599	**37,989**
Switzerland	400					200	10,264	495	1,220		**12,580**

Storage

Conventional storage (pumped storage, hydroelectric generation with reservoir, batteries, compressed and liquid air energy storage) and demand-side response (DSR: load shifting and peak shaving) are modelled (see Table A. *5*). All storage and DSR assumptions are taken from ESO (2024) and ENTSOe (2024). Hydro energy inflow data, discharge and charge capacities for the modelled market zones are derived from the Pan-European Market Modelling Database (PEMMDB),[11] part of the *ERAA2023* study. Hydro inflows are sourced from the "Storage_technology - Year Dependent" sheet in the files accessible via the Hydro Inflows ZIP, with the reference year set to 1998 under normal climatic conditions. Discharge, charge, and volume capacities are obtained from the sheet "TY2030" in ERAA 2023 PEMMDB Generation.xlsx.

Assumptions and data processing for hydro and PS technologies:

- Zones with positive discharge capacity but zero volume capacity assume discharge capacity equals volume capacity.
- Efficiency losses for pumped storage are assumed to be 25%.

Battery and DSR discharge, charge, and volume capacities are primarily based on ESO (2024), supplemented by ERAA 2023 PEMMDB Generation.xlsx for non-GB zones. DSR capacities for Great Britain (GB) are sourced from FES, while for other regions, data is derived from the "TY2030" in ERAA 2023 PEMMDB Generation.xlsx. Note that we take hydro generation capacity from the PEMMDB dataset. In particular, according to the PEMMDB dataset, GB has 2,219.5 MW of hydro-run-of-river generation capacity with storage capability (pondage).

Assumptions and data processing for batteries and DSR:

- GB DSR capacity values are exclusively based on FES, while other zones use PEMMDB data.
- Battery storage calculations are based on the injection/offtake ratio in TYNDP, assuming 3 hours of energy storage for zones without specific data.
- Round-trip efficiency losses for batteries are assumed to be 15%.
- Implicit (load shifting) DSR assumes a uniform 4-hour "storage" (or shifting) capacity.
- Peak shaving is modelled in great detail following assumptions on price bands, capacity and availability hours, according to ERAA 2023 PEMMDB.

According to FES HE 2030, GB's total consumer DSR (residential, industrial, and commercial consumers) may provide up to 2.07 GW of demand reduction at its peak in 2030 (in 2023, this is 1.24 GW, according to FES HE). Further, FES HE 2030 assumes 8.16 GW of demand flexibility from smart charging (1.97 GW) and flexibility from domestic and industrial heat storage, hybrid heat pumps and thermal storage (in 2023, this is 6.04 GW, according to FES HE). Thus, in the FES HE scenario, GB is projected to have 10.22 GW of demand-side flexibility by 2030. Overall, this flexibility level is rather ambitious and sits at the high end of forecasts from other stakeholders and institutions (e.g., according to Torriti (2024), Carbon Trust and Imperial College London forecast optimal DSR capacity to be between 4.1 GW and 11.4 GW by 2030). Our dispatch model assumes 2.07 GW of implicit DSR (load shifting) and another 6.19 GW of peak shaving (taken from ERAA 2023 PEMMDB), totalling 8.25 GW of DSR for GB by 2030. Note that peak shaving capacity will unlikely help reduce curtailment. They are designed to reduce peak-hour demand rather than to provide intertemporal flexibility to shift the residual load and reduce curtailment.

FES reports capacity for Compressed Air and Liquid Air Storage for GB only. Thus, their discharge, charge and volume capacities for compressed air and liquid air storage are derived from FES data. Data for these storage technologies from other regions is unavailable.

[11] https://eepublicdownloads.blob.core.windows.net/public-cdn-container/clean-documents/sdc-documents/ERAA/2023/ERAA2023%20PEMMDB%20Generation.xlsx

Table A. 5: Electricity storage and demand side response capacity in 2030

	Conventional storage		DSR	
	Discharge, MW	**Duration*, hours**	**Discharge, MW**	**Duration*, hours**
Austria	16,463	125	1,400	14
Belgium	2,130	3	10,107	11
Czech Republic	4,105	3		
Denmark	364	8		
Finland	4,030	571	4,641	4
France	28,588	152	9,999	11
Germany	32,652	49	6,722	5
GB1	369	2	42	4
GB2	5694	3	105	4
GB3	883	2	95	4
GB4	9,397	5	369	4
GB5	7,182	2	1,159	4
GB6	319	2	42	4
GB7	2,504	2	253	4
Island of Ireland	2,179	3	667	4
Italy	25,431	134	2,286	4
Luxembourg	62	1	90	5
Netherlands	2,362	2	1,687	4
Norway	36,303	4,786	19,713	7
Poland	3,607	2		
Portugal	8,598	271		
Slovenia	1,399	8	110	13
Spain	25,590	527	2,000	4
Sweden	16,826	1,024	3,478	19
Switzerland	18,029	303		

Notes: * average for all storage technologies

Assumptions and data processing for Compressed Air and Liquid Air Storage:

- The installed capacities for compressed and liquid air storage reported in the FES databook are treated as discharge and charge capacities, respectively.
- Discharge durations for zones without specific data are assumed to be 3 hours for compressed air[12] and 5 hours for liquid air (Vecchi et al., 2021).
- Round-trip efficiency is assumed to be 57.5% for both technologies, corresponding to the midpoint of the 45-70% range reported by Vecchi et al. (2021).

Network

The network data for interconnections (IC) between zones in the model includes Net Transfer Capacities (NTCs), their assumed hourly availability profiles, and associated losses. The primary source for this data is the Pan-European Market Modelling Database (PEMMDB), specifically the file PEMMDB_Transfer_Capacities_2030.xlsx, which contains information on both HVDC and HVAC lines for European market zones. Supplementary data was drawn from FES, Ofgem[13] and public sources to calculate interconnections between GB zones and the rest of Europe.

To create the interconnector data, only interconnections where both connected nodes are listed within the relevant zones were included in the analysis. The NTC values for these interconnections were derived directly from their rated power. The interconnection availability profiles were assumed to be 1

[12] https://www.modernpowersystems.com/analysis/compressed-and-liquid-air-for-long-duration-high-capacity-11065946/

[13] https://www.ofgem.gov.uk/energy-policy-and-regulation/policy-and-regulatory-programmes/interconnectors

(i.e., available at all hours). Where multiple interconnections existed between the same zones, they were categorised as additional lines. By 2030, GB is projected to have 14,514 MW of interconnection capacity with the rest of Europe:

1. 2,400 MW with Belgium (NEMO with 1000 MW connected to GB7 and Chronos with 1400 MW connected to GB5)
2. 1,400 MW with Germany (Neuconnect with 1400 MW connected to GB5)
3. 1,400 MW with Denmark (Viking Link with 1400 MW connected to GB5)
4. 1000 MW with the Netherlands (Britned with 1000 MW connected to GB5)
5. 1,464 MW with Norway (NSL with 1464 MW connected to GB3)
6. 1,450 MW with the Island of Ireland (Moyle with 450 MW connected to GB2, EWIC with 500 MW connected to GB4, and GreenLink with 500 MW connected to GB5)
7. 5,400 MW with France (IFA1 and IFA2 with 3000 MW connected to GB7, ElecLink with 1000 MW connected to GB7, and Gridlink with 1400 MW connected to GB5)

In 2023, GB's total interconnection capacity was 8464 MW. The final dataset includes the processed NTC values and interconnections availability profiles, incorporating the adjustments for GB sub-zones. Zones Z2, Z4, and Z5 are connected to the SEM; Z5 is also connected to BE, DE, DK, FR, and NL. Z7 is also connected to FR.

Costs and prices

Load curtailment cost is assumed to be €4,000/MWh-e, which aligns with the ERAA 2023 price cap assumption. Carbon prices for the GB and European power markets are assumed to be €107/tCO2 and €86/tCO2, respectively.[14] Fuel prices were sourced from FES 2024 (taking 2023 gas, coal and oil prices) and from the BEIS (2023) Electricity Generation Costs 2023 report (Table A. 6).

Table A. 6: Assumed fuel prices

	€2023 per MWh-th
Coal	14.52
Oil	53.69
Gas	40.42
Dedicated biomass	11.83
Biomass CHP	14.64
Biomass CCS*	22.02

Notes: * BEIS (2020) and ESO (2024) for coal, oil and gas prices

Assumed avoidable (variable non-fuel) cost for exogenous generation (non-dispatchable generation) was assumed as follows:

1. Other RES: €40.53/MWh-e.
2. Wave energy: €26.69/MWh-e;
3. Landfill gas: €14.83/MWh-e;
4. Hydroelectric; €10.38/MWh-e;
5. Wind onshore: €8.90/MWh-e;
6. Wind offshore: €1.48/MWh-e;
7. Solar PV: €0/MWh-e;
8. Nuclear: -€10 /MWh-e.

[14] These carbon price levels were observed in 2023, based on *FES 2024*

It should be noted that the nuclear avoidable cost is an artificial construct designed to ensure that the dispatch model curtails nuclear power only as a last resort. This assumed variable (non-fuel) cost structure prioritises curtailing other renewable energy sources (RES) first, treating them as the most expensive, while solar PV and nuclear power are curtailed last. When solar PV is curtailed, the shadow price of the demand-supply constraint (system marginal cost) will be zero. However, if nuclear power is also curtailed, this value could drop to negative €10. An alternative approach to ensuring nuclear has minimal curtailment is to require longer up-and-down times and very low ramp rates. However, these features require explicit unit commitments imposed on nuclear, which can be modelled, but at the cost of increased computational complexity. There is evidence in the offer and bid prices that EDF Energy Nuclear Generation makes into the Balancing mechanism - e.g., on 19/08/25, all stations had a spread from £10,000 to -£10,000/MWh, indicating their unwillingness to flex at short notice.ss

Data and Appendix References

Ah-Voun, D., Chyong, C. K., & Li, C. (2024). Europe's energy security: From Russian dependence to renewable reliance. *Energy Policy*, 184, 113856. https://doi.org/10.1016/j.enpol.2023.113856

ENTSOE, 2023. *ERAA 2023 Study*, https://eepublicdownloads.blob.core.windows.net/public-cdn-container/clean-documents/sdc-documents/ERAA/2023/ERAA2023%20PEMMDB%20Generation.xlsx .

ESO, 2024a. *Future Energy Scenarios*, https://www.neso.energy/publications/future-energy-scenarios-fes

ESO, 2024b. *Future Energy Scenarios Data Book*, at https://www.neso.energy/fes-data-workbook-2024

Jacobson, M.Z., & Jadhav, V. (2018). World estimates of PV optimal tilt angles and ratios of sunlight incident upon tilted and tracked PV panels relative to horizontal panels. *Solar Energy*, 169, 55-66.

PECD 2021. *Pan-European Climatic Database* (PECD 2021.3) https://zenodo.org/records/7224854

Pfenninger, P. & I. Staffell, 2016. Using bias-corrected reanalysis to simulate current and future wind power output, *energy*, 114, 1224-1239, https://doi.org/10.1016/j.energy.2016.08.068 .

Pfenninger, P. & I. Staffell, 2016. Long-term patterns of European PV output using 30 years of validated hourly reanalysis and satellite data, *energy*, 114, 1251-1265, https://doi.org/10.1016/j.energy.2016.08.060

TYNDP, 2022. *Ten Year Network Development Plan*, https://2022.entsos-tyndp-scenarios.eu/wp-content/uploads/2022/04/TYNDP_2022_Scenario_Building_Guidelines_Version_April_2022.pdf

Torriti, J. (2024). Governance perspectives on achieving demand side flexibility for net zero. *Energy Policy*, 191, 114148.

Vecchi, A., Li, Y., Ding, Y., Mancarella, P., & Sciacovelli, A. (2021). Liquid air energy storage (LAES): A review on technology state-of-the-art, integration pathways, and future perspectives. *Advances in Applied Energy*, 3, 100047.

Appendix 2: Additional results

Table A. 7 shows the full impact of increasing each VRE one zone at a time. The table shows that even for expansions far from Z1 and Z2, most of the curtailment occurs in those zones.

Table A. 7: Full zonal impact of individual VRE increments

Individual expansions		Z1	Z2	Z3	Z4	Z5	Z6	Z7	Total
OFF Curtailment, GWh	Z1	38	14	1	1	2	0	1	57
	Z2	28	16	1	1	2	-0	1	48
	Z3	6	10	1	1	2	0	0	20
	Z4	37	38	4	3	2	0	1	84
	Z5	11	21	2	2	3	0	1	39
	Z6	36	30	4	3	7	0	1	80
	Z7	10	8	1	1	2	0	0	22
ON curtailment, GWh	Z1	240	7	0	0	1	-0	0	249
	Z2	176	161	1	0	0	-0	0	339
	Z3	1	5	8	-0	2	-0	0	15
	Z4	12	11	1	17	-1	-0	0	39
	Z5	9	16	2	1	18	0	1	48
	Z6	-7	1	0	0	0	2	-0	-3
	Z7	1	2	0	0	-1	-0	4	6
PV Curtailment, GWh	Z1	2	5	0	0	2	0	0	10
	Z2	5	2	0	0	2	0	-0	9
	Z3	5	3	1	0	1	0	0	11
	Z4	5	14	1	1	0	1	1	22
	Z5	48	45	5	7	6	1	3	115
	Z6	9	3	1	0	-0	-0	0	13
	Z7	16	15	3	1	2	0	1	38

Table A. 8: Impact of expanding VRE in Z5 with high EU VRE

High VRE		Z1	Z2	Z3	Z4	Z5	Z6	Z7	Total	normal	delta
curtailment	OFF	8	28	4	7	5	2	2	56	39	44%
GWh	ON	7	26	3	10	34	1	2	83	48	72%
	PV	51	75	13	17	7	3	5	172	115	50%

Table A. 8 shows that at the level of individual expansions in the central part of the country (Z5), High EU VRE increases curtailment by 44%-72%.

Table A. 9: Levelised marginal costs of VRE, £(2024)/MWh

	Z1	Z2	Z3	Z4	Z5	Z6	Z7
OFF	£95.36	£83.64	£51.48	£44.16	£37.39	£45.87	£41.32
ON	£102.46	£84.74	£48.29	£43.67	£37.02	£35.73	£37.89
PV grid-scale	£93.87	£77.52	£50.05	£46.29	£38.91	£43.40	£37.97
PV mid-scale	£165.62	£146.37	£102.36	£99.35	£88.73	£92.74	£81.97

Table A. 10: Levelised average cost of VRE, £2024/MWh

	Z1	Z2	Z3	Z4	Z5	Z6	Z7
OFF	£73.06	£58.73	£43.49	£37.02	£31.86	£38.43	£34.71
ON	£66.94	£53.13	£40.16	£35.05	£30.58	£35.76	£33.71
PV grid-scale	£75.36	£61.09	£44.41	£41.84	£34.32	£36.01	£34.18
PV mid-scale	£132.97	£115.35	£90.82	£89.79	£78.27	£76.95	£73.78

Appendix 3: Mathematical formulation of the UCED model

The model is an extension of two models: (i) the unit commitment and economic dispatch model developed by Chyong and Newbery (2022) for the GB electricity market, and (ii) the Pan-European electricity dispatch model developed by Chyong et al. (2019). The main extension includes:

1. Joint dispatch of electricity and hydrogen;
2. Endogenous dispatch of hydropower with energy inflow and storage capability;
3. Explicit and implicit demand-side response;
4. Improvements to the storage and interconnector modelling, in particular, handling issues related to simultaneous flows and improvements to the ramp limits for interconnectors;
5. Nodal market design, including nodal line flow modelling and LMP computations;
6. Handling of time-dependent input parameters for generation, storage and transmission.

The rest of this section presents a mathematical formulation of the new model version, while Appendix 1 outlines the data sources and assumptions used to generate the model inputs. We start with model notations first and then outline its equations.

Notation

This section gives details about symbols used in our unit commitment model. For clarity of presentation, all exogenous parameters are written in lowercase. Decision variables are capitalised, whereas auxiliary variables are written in lowercase and *italicised*. Subscripts are used for indexation, while superscripts are used to clarify the meaning of variables and parameters when necessary.

Sets and Indices

$t, tt \in T$	Set of all time periods in a modelling horizon *r;*
$r, rr \in R$	Set of all rolling horizons;
$j, jj \in J$	Set of all generators, semi-endogenous interconnectors and storage units in the model; $j \in J(f)$ - subset of all thermal generation units; $j \in J(s)$ - subset of all storage units; $j \in J(i)$ - subset of all semi-endogenous interconnectors where *i* denotes an external market; $j \in J(v)$ - subset of all variable renewable electricity (VRE) generation units (wind and solar).

Decision Variables

Name	Description/Comment	Unit
Binary Variables		
PLANT_COMMIT(r, t, j)	Commitment status of a thermal plant $j \in J(f)$ at time *t*. 1 - committed, otherwise 0; the unit commitment feature for unit j can be switched on by setting uc_flag$(j) = 1$ or off by setting this parameter to 0.	n.a.
PLANT_START(r, t, j)	Start-up status of a thermal plant $j \in J(f)$ at time *t*. 1 - the unit *j* starts up, otherwise 0	n.a.
PLANT_SHUT(r, t, j)	Shut-down status of a thermal plant $j \in J(f)$ at time *t*. 1 - the unit *j* shuts down, otherwise 0	n.a.
STOR_CHRG_COMMIT(r, t, j)	Commitment status of a storage unit $j \in J(s)$ at time *t*. 1 -committed to charge, otherwise 0	n.a.

IZFLOW_COMMIT(r, t, n, k, nn)	Binary variable indicating whether the interzonal flow for line *k* is committed between nodes *n* and *nn* at time *(r,t)*. This ensures mutual exclusivity of forward and backward flows.	n.a.
EXT_IC_COMMIT(r, t, j)	A binary variable indicating whether (semi-endogenous) interconnector *j(i)* is in importing mode (=1) or export mode (=0).	n.a.

Continuous Decision Variables (Electricity)

FUEL_CONS_POWER(r, t, f, j)	The fuel consumption of generation technology *j* using fuel *f* at node *n* and time *(r,t)*.	MWh-th
SPINUP(r, t, j)	Represents the spinning up reserve provided by generation unit j at time *(r,t)*	MW
NS_SPINUP(r, t, j)	Represents the non-spinning reserve contribution by generation unit j at time *(r,t)*	MW
STOR_SPINUP(r, t, j)	Represents the reserve contribution from storage units in discharge mode at time *(r,t)*	MW
SPINDOWN(r, t, j)	Represents the spinning down reserve provided by generation unit j at time *(r,t)*	MW
STOR_SPINDOWN(r, t, j)	Represents the reserve contribution from storage units in charging mode (spinning down) at time *(r,t)*	MW
EXT_IC_IMP(r, t, j)	Electricity import flow through (semi-endogenous) interconnector j at time *(r,t)*	MWh
EXT_IC_EXP(r, t, j)	Electricity export flow through (semi-endogenous) interconnector j at time *(r,t)*	MWh
E_IZ_FLOW(r, t, n, k, nn)	The decision variable representing interzonal electricity flow between nodes *n* and *nn* over line *k* at time *(r,t)*	MWh
STOR_CHRG(r, t, j)	Represents the energy charged into storage *j* at time *(r,t)*	MWh
STOR_DCHRG(r, t, j)	Represents the energy discharged from storage *j* at time *(r,t)*	MWh
DEM_E_CURT(r, t, n)	Represents electricity demand curtailed at node *n* at time *(r,t)*	MWh
HYDRO_E_CURT(r, t, n)	Represents curtailment of hydro inflow at time *(r,t)*	MWh

Continuous Decision Variables (Hydrogen)

H2_ELEC_PWR_CONS(r, t, j)	Power consumed (in MWh-e) by hydrogen electrolyser *j* at time *(r,t)*	MWh
H2_IZ_FLOW(r, t, n, k, nn)	Represents the hydrogen flow from node *n* to node *nn* through pipeline *k* at time *(r,t)*	MWh-th

$\mathrm{H2\_STOR\_CHRG(r,t,j)}$	Represents the amount of hydrogen charged into storage unit *j* at time *(r,t)*	MWh-th
$\mathrm{H2\_STOR\_DCHRG(r,t,j)}$	Represents the amount of hydrogen discharged from storage unit *j* at time *(r,t)*	MWh-th
$\mathrm{H2\_DEM\_CURT_{r,t,n}}$	Represents hydrogen demand curtailed at node *n* at time *(r,t)*	MWh-th
Auxiliary Variables		
$power\_out(r,t,j)$	Electrical energy output of a unit $j \in J(f)$ at time *(r,t)*, defined as follows: $$power\_out(r,t,j) = \sum_f \mathrm{FUEL\_CONS\_POWER}(r,t,f,j) \cdot \mathrm{thermal\_eff}(f,j)$$	MWh
$vre\_curtail(r,t,j)$	Curtailment of variable renewable electricity (VRE) technology *j* (wind and solar) at time *(r,t)*, defined as follows: $$vre\_curtail(r,t,j) = \mathrm{max\_pwr\_out(r,t,j)} - power\_out(r,t,j)$$	MWh
$ext\_ic\_net\_flow(r,t,j)$	Represents (semi-endogenous) external net electricity imports (positive) less exports (negative) through interconnectors *j* at time *(r,t)*, defined as follows: $$ext\_ic\_net\_flow(r,t,j) = \mathrm{EXT\_IC\_IMP(r,t,j)} - \mathrm{EXT\_IC\_EXP(r,t,j)}$$	MWh
$ramp\_up(r,t,j)$	Represents the ramp-up decision for unit *j* at time *(r,t)*, defined as follows: $$ramp\_up(r,t,j) = power\_out(r,t,j) - power\_out(r,t-1,j)$$	MWh
$ramp\_down(r,t,j)$	Represents the ramp-down decision for unit *j* at time *(r,t)*, defined as follows: $$ramp\_down(r,t,j) = power\_out(r,t-1,j) - power\_out(r,t,j)$$	MWh
$nodal\_net\_energy\_inj(r,t,n)$	Represents net nodal energy injection (used only for the nodal market design problem) at node n and time *(r,t)*, defined as follows:	MWh

$$
\begin{aligned}
&nodal\_net\_energy\_inj(r,t,n) \\
&\quad = \sum_{j(n)} power\_out(r,t,j) \\
&\quad \cdot (1 - \text{eff\_loss}(j)) \\
&\quad + \sum_{j(n)} \text{STOR\_DCHRG}(r,t,j) \\
&\quad + \sum_{j(n)} ext\_ic\_net\_flow(r,t,j) \\
&\quad \cdot (1 - \text{eff\_loss}(j)) \\
&\quad + \sum_{(nn,k)} [\text{E\_IZ\_FLOW}(r,t,nn,k,n) \\
&\quad - \text{E\_IZ\_FLOW}(r,t,n,k,nn)] \\
&\quad - [\text{demand\_e}(r,t,n) \\
&\quad - \text{DEM\_E\_CURT}(r,t,n)] \\
&\quad - \sum_{j(n)} \text{STOR\_CHRG}(r,t,j)
\end{aligned}
$$

$nodal\_line\_flow(r,t,k)$	Represents net nodal energy injection (used only for the nodal market design problem) at node n and time *(r,t)*, defined as follows: $$nodal\_line\_flow(r,t,k) = \sum_{n} nodal\_net\_energy\_inj(r,t,n) \cdot \text{nodal\_reduced\_PTDF}(n,k)$$	MWh
$storage\_level(r,t,j)$	Represents storage level for unit *j* (electricity) at time *(r,t)*, defined as follows: $$\begin{aligned} storage\_level(r,t,j) &= storage\_level(r,t-1,j) \\ &+ [\text{stor\_hydro\_inflow}(r,t,j) \\ &- \text{HYDRO\_CURT}(r,t,j)] \\ &+ [\text{STOR\_CHRG}(r,t,j) \\ &\cdot (1 - \text{eff\_loss}(j)) \\ &- \text{STOR\_DCHRG}(r,t,j)] \end{aligned}$$	MWh
$FuelStock\_level(r,t,f,j)$	Represents fuel stock level of unit *j* and fuel *f* at time *(r,t)*, defined as follows: $$\begin{aligned} \text{FuelStock\_level}(r,t,f,j) &= \text{fuel\_stock\_init}(f,j) \\ &- \text{FUEL\_CONS\_POWER}(r,t,f,j) \end{aligned}$$	MWh-th
$FlowChange\_BW\_FW(r,t,k)$	An auxiliary binary variable representing a change in flow direction from backwards to forward direction over line *k* at time *(r,t)*	n.a.

$FlowChange\_FW\_BW(r,t,k)$	An auxiliary binary variable representing a change in flow direction from forward to backwards direction over line *k* at time *(r,t)*	n.a.
$H2\_output(r,t,j)$	The quantity of hydrogen produced by technology *j* in node *n* at time *(r,t)*, defined as follows: $\text{H2\_output}(r,t,j) = \text{H2\_ELEC\_PWR\_CONS}(r,t,j) \cdot \text{H2\_elec\_eff}(j)$	MWh-th
$H2\_Storage\_level(r,t,j)$	Represents the hydrogen volume held in storage unit *j* at time *(r,t)*, defined as follows: $\text{H2\_Storage\_level}(r,t,j) = \text{H2\_Storage\_level}(r,t-1,j) + \text{H2\_STOR\_CHRG}(r,t,j) \cdot (1-\text{eff\_loss}(j)) - \text{H2\_STOR\_DCHRG}(r,t,j)$	MWh-th
Input Parameters (Electricity)		
demand_e(r, t, n)	Electricity demand input at node *n* and time *(r,t)*	MWh
spinup_res(r, t, n)	Spinning up reserve requirement at node *n* and time *(r,t)*	MW
spindown_res(r, t, n)	Spinning down reserve requirement at node *n* and time *(r,t)*	MW
snsp_lim(n)	Non-synchronous penetration (SNSP) limit for node n; set as a ratio of demand at node n	Unitless
fuel_map(f,j)	A binary parameter that maps fuel f to technology j	n.a.
gen_type(j)	A classification parameter [1- generation; 2 - storage; 3-external (semi-endogenous interconnectors]	n.a.
eff_loss(j)	Loss of energy output associated with parasitic load at a generation plant j. For storage, this is loss due to mechanical or chemical processes.	unitless
max_pwr_out(r,t,j)	Maximum generation for unit j at time (r,t)	MW
min_pwr_out(r,t,j)	Minimum stable generation level for unit j at time (r,t)	MWh
ramp_up_rt(j)	Ramp-up rate of unit j	MW/time step
ramp_down_rt(j)	Ramp-down rate of unit j	MW/time step
ramp_trans_ext_ic(j)	Transition ramp rate for external IC (semi-endogenous), defined as min(ramp_up_rt(j),ramp_down_rt(j))	MW/time step

thermal_eff(f,j)	Thermal efficiency of unit j using fuel f	MWh-e/MWh-th
carbon_intensity(f,j)	Carbon intensity of technology j using fuel f	tCO2/MWh-e
init_fuel_stock(f,j)	Fuel stock of fuel type f available to technology j at the beginning of the modelling horizon	MWh-th
min_uptime(j)	minimum up time of technology j	Time step
min_downtime(j)	minimum downtime of technology j	Time step
L(j)	downtime before the start of the modelling horizon	Time step
G(j)	uptime before the start of the modelling horizon	Time step
stor_init_stock(j)	initial energy hold in stock for electricity storage j	MWh
stor_vol_cap(j)	storage volume capacity	MWh
stor_dchrg_cap(r,t,j)	The storage discharge capacity of unit *j* at time *(r,t)*	MW
stor_chrg_cap(r,t,j)	The storage charge capacity of unit *j* at time *(r,t)*	MW
stor_hydro_inflow(r,t,j)	The energy available for hydro unit *j* and explicit demand-side response (peak shaving) at time *(r,t)*	MWh
fuel_flow(r,t,f,n)	Fuel type f supply to node n at time (r,t)	MWh-th
nodal_PTDF(n,k)	Power transfer distribution factor. This parameter is applied only to the formulation of the nodal model.	Unitless
nodal_line_cap(r,t,k)	Line *k* capacity at time (r,t); This parameter is applied only to the formulation of the nodal model.	MW
nodal_line_resistance(k)	Resistance of line *k*; This parameter is applied only to the formulation of the nodal model.	p.u.
nodal_iface_cap(i)	Interface (a collection of lines k) *i*'s capacity; This parameter is applied only to the formulation of the nodal model.	MW
nodal_line_direction(k)	Interface *i*'s direction (1- forward; -1 - backwards); This parameter is applied only to the formulation of the nodal model.	n.a.
iz_line_cap(r,t,n,k,nn)	Interzonal line *k* capacity at time *(r,t)*, connecting nodes *(n,nn)*	MW
iz_line_ramp(n,k,nn)	Ramp rate for line k	MW/time step
iz_line_ramp_bw_fw(k)	The transition ramp rate for line *k* when changing flows from backwards to forward is defined as a lesser of the two ramp rates (*n* to *nn*, forward direction and *nn* to *n*, backward direction).	MW/time step

iz_line_ramp_fw_bw(k)	The transition ramp rate for line *k* when changing flows from forward to backwards is defined as a lesser of the two ramp rates (*n* to *nn*, forward direction and *nn* to *n*, backward direction).	MW/time step
carbon_price(r,t,n)	Carbon price applied at node n and time (r,t)	$/tCO2
demand_curt_cost(n)	Electricity load shedding cost at node n	$/MWh
iz_line_varcost(n,k,nn)	Short-run variable cost of flow over line *k*	$/MWh
fuel_cost(r,t,f)	Supply cost of fuel *f* at time *(r,t)*	$/MWh-th for thermal sources and $/MWh-e for electricity sources
varcost(r,t,j)	Short-run variable cost of unit *j* at time *(r,t)*	$/MWh
start_cost(j)	Start-up cost of unit j	$/start
shut_cost(j)	Shut down cost of unit j	$/shut
ramp_up_cost(j)	Ramp-up cost of unit j	$/MWh/time step
ramp_down_cost(j)	Ramp-down cost of unit j	$/MWh/time step
spin_up_cost(j)	Spin-up reserve cost provided by unit j	$/MW
capcost_res_up(n)	The unit cost associated with upward reserve capacity shortfalls for node n	$/MW
capcost_res_down(n)	The unit cost associated with downward reserve capacity shortfalls for node n	$/MW
capcost_LB(j)	Cost associated with lower bound violations	$/MWh-e
capcost_UB(j)	Cost associated with upper bound violations	($/MW-e
capcost_rampup(j)	Cost associated with ramp-up limit violations	$/MWh-e/time step
capcost_rampdown(j)	Cost associated with ramp-down limit violations	$/MWh-e/time step
capcost_line_flow(k)	Cost per unit of forward or backward flow capacity violation for line k	$/MW
capcost_iface_flow(i)	Per-unit penalty cost associated with interface flow capacity violations (forward or backward) for interface *i*	$/MW
Input Parameters (Hydrogen)		
H2_demand(r,t,n)	Hydrogen demand at node *n* and time *(r,t)*	MWh-th

H2_elec_cap(r,t,j)	Electrolysis j's capacity at time (r,t)	MW-e
H2_elec_ramp_up(j)	Electrolysis j's ramp-up capacity	MW-e/time step
H2_elec_ramp_down(j)	Electrolysis j's ramp-down capacity	MW-e/time step
H2_elec_eff(j)	Electrolysis j's conversion efficiency	MWh-th/MWh-e
H2_stor_init_stock(j)	Initial energy available in stock in hydrogen storage j	MWh-th
H2_stor_vol_cap(j)	Hydrogen storage j capacity	MWh-th
H2_stor_chg_cap(r,t,j)	Hydrogen storage j charge capacity at time *(r,t)*	MWh-th
H2_stor_dchg_cap(r,t,j)	Hydrogen storage j discharge capacity at time *(r,t)*	MWh-th
H2_iz_line_cap(r,t,n,k,nn)	Hydrogen pipeline k's capacity at time *(r,t)*	MWh-th
H2_iz_line_loss(k)	Hydrogen pipeline k's line loss (as a fraction of energy transported)	unitless
H2_demand_curt_cost(n)	Hydrogen demand curtailment cost at node n	$/MWh-th
H2_price(r,t,n)	Hydrogen price at node n and time (r,t)	$/MWh-th
H2_varcost(r,t,j)	Hydrogen unit j's short-run variable cost	$/MWh-th
H2_iz_line_varcost(n,k,nn)	Hydrogen pipeline k's variable cost	$/MWh-th

Electricity dispatch module

System constraints

The balancing electricity supply and demand constraint (eq.A1) ensures that electricity supply matches demand within zonal electricity systems when the model operates in zonal mode. It integrates supply components, including generation, storage discharge, net interconnector imports (semi-endogenous), and interzonal flows (all adjusted for efficiency losses), with electricity demand, curtailment, and storage charging. The constraint maintains balance at every node by accounting for physical and efficiency losses. Its shadow price reflects the marginal cost of meeting incremental electricity demand, serving as a key indicator of marginal supply cost, potential supply constraints and system capacity limitations within a zone.

$$\begin{aligned}\forall r,t,n:\ &\sum_{j(n)} power\_out(r,t,j)\cdot\left(1-\text{eff\_loss}(j)\right)+\sum_{j(n)}\text{STOR\_DCHRG}(r,t,j)\\&+\sum_{j(n)} ext\_ic\_net\_flow(r,t,j)\cdot\left(1-\text{eff\_loss}(j)\right)\\&+\sum_{(nn,k)}\text{E\_IZ\_FLOW}(r,t,nn,k,n)\cdot\left(1-\text{iz\_line\_loss}(k)\right)\\&=\text{demand\_e}(r,t,n)-\text{DEM\_E\_CURT}(r,t,n)\\&+\sum_{j(n)}\text{STOR\_CHRG}(r,t,j)+\sum_{(nn,k)}\text{E\_IZ\_FLOW}(r,t,n,k,nn)\end{aligned}\qquad\text{(A1)}$$

Equation A2 ensures a total balance between electricity supply and demand across all nodes in the nodal model configuration. It accounts for local generation, storage discharge, and interconnector imports (all adjusted for efficiency losses) to meet aggregated electricity demand, storage charging, and curtailment. Its shadow price captures the marginal cost of meeting incremental total electricity demand. This is a key component in calculating locational marginal prices (LMP) at the node level.

$$\begin{aligned}\forall r,t:\ &\sum_{(j,n)} power\_out(r,t,j)\cdot\left(1-\text{eff\_loss}(j)\right)+\sum_{(j,n)}\text{STOR\_DCHRG}(r,t,j)\\ &+\sum_{(j,n)} ext\_ic\_net\_flow(r,t,j)\cdot\left(1-\text{eff\_loss}(j)\right)\\ &=\sum_{n}\left[\text{demand\_e}(r,t,n)-\text{DEM\_E\_CURT}(r,t,n)\right]\\ &+\sum_{(j,n)}\text{STOR\_CHRG}(r,t,j)\end{aligned} \tag{A2}$$

The spinning-up reserve constraint (eq.A3) ensures that spinning reserve requirements at a node are met through contributions from spinning reserves (active generation units), non-spinning reserves (offline units capable of rapid activation), and storage units in discharge mode. An artificial variable (*capacity_res_up*(r,t,n)) allows for unmet reserve requirements at a high penalty cost, aiding infeasibility management. The shadow price of this constraint reflects the marginal cost of fulfilling additional reserve requirements, highlighting reserve capacity constraints or the need for greater system flexibility.

$$\begin{aligned}\forall r,t,n:\ &\sum_{j(n)}\text{SPINUP}(r,t,j)+\sum_{j(n)}\text{NS\_SPINUP}(r,t,j)+\sum_{j(n)}\text{STOR\_SPINUP}(r,t,j)\\ &\geq \text{spinup\_res}(r,t,n)-capacity\_res\_up(r,t,n)\end{aligned} \tag{A3}$$

The spinning down reserve constraint (eq.A4) ensures that spinning down reserve requirements at a node are met through contributions from generation units capable of rapidly reducing output and storage units in charging mode. An artificial variable (*capacity_res_down*(r,t,n)) permits constraint relaxation at a high penalty cost to manage infeasibility. The shadow price of this constraint indicates the marginal cost of meeting additional reserve requirements, with high values signalling tight reserve capacity or shortfalls that are penalised through the relaxation mechanism.

$$\begin{aligned}\forall r,t,n:\ &\sum_{j(n)}\text{SPINDOWN}(r,t,j)+\sum_{j(n)}\text{STOR\_SPINDOWN}(r,t,j)\\ &\geq \text{spindown\_res}(r,t,n)-capacity\_res\_down(r,t,n)\end{aligned} \tag{A4}$$

The system non-synchronous penetration constraint (eq.A5) limits the share of non-synchronous generation (e.g., wind, solar) and electricity imports at a node to a specified fraction of total electricity demand, interzonal inflows, storage charging, and hydrogen electrolysis consumption. This constraint ensures grid stability by accounting for technical limitations to integrating variable renewable energy. The constraint applies exclusively to zonal model formulations, balancing demand and flows at the aggregated zone level.

$$\forall r,t,n: \sum_{j(n)\in J(v)} power\_out(r,t,j) + \sum_{(nn,k)} \text{E\_IZ\_FLOW}(r,t,nn,k,n) \leq \text{snsp\_lim}(n) \cdot \left[\text{DEMAND\_E}(r,t,n) + \sum_{(nn,k)} \text{E\_IZ\_FLOW}(r,t,n,k,nn) + \sum_{j(n)} \left(\text{STOR\_CHRG}(r,t,j) + \text{H2\_ELEC\_PWR\_CONS}(r,t,j)\right)\right] \quad \text{(A5)}$$

Generation constraints

Considering operational decisions and reserve contributions, the minimum stable generation constraint (eq. A6) ensures that power output from a generation unit meets or exceeds its minimum stable generation level. An artificial variable (*capacity_power_LB*(r,t,j)) permits constraint relaxation at a high penalty cost to handle potential infeasibilities.

The maximum generation constraint (eq. A7) ensures that the total power output of a generation unit, including spinning reserve contributions, does not exceed its defined capacity. This constraint includes an artificial variable (*capacity_power_UB*(r,t,j), allowing for relaxation at a high penalty cost if necessary.

$$\begin{aligned}\forall r,t,j: & \; power\_out(r,t,j) \\ & \geq [\text{PLANT\_COMMIT}(r,t,j) \cdot \text{min\_pwr\_out}(r,t,j)] \\ & + \text{min\_pwr\_out}(r,t,j) + \text{SPINDOWN}(r,t,j) \\ & - capacity\_power\_LB(r,t,j)\end{aligned} \quad \text{(A6)}$$

$$\begin{aligned}\forall r,t,j: & \; power\_out(r,t,j) + \text{SPINUP}(r,t,j) \\ & \leq [\text{PLANT\_COMMIT}(r,t,j) \cdot \text{max\_pwr\_out}(r,t,j)] \\ & + \text{max\_pwr\_out}(r,t,j) \cdot \left(1 - \text{uc\_flag}(j)\right) \\ & + capacity\_power\_UB(r,t,j)\end{aligned} \quad \text{(A7)}$$

The ramp-up (eq. A8) and ramp-down (eq. A9) constraints ensure that the change in power output of generation units between consecutive time steps does not exceed their defined ramp limits, incorporating operational conditions and spinning reserve contributions. These constraints include artificial variables on the right-hand side to relax the upper bound at a high penalty cost if unmet ramp limit requirements occur.

$$\begin{aligned}\forall r,t,j: & \; ramp\_up(r,t,j) + \text{SPINUP}(r,t,j) \\ & \leq [\text{min\_pwr\_out}(r,t,j) \\ & \cdot \left(2 - \text{PLANT\_COMMIT}(r,t,j) - \text{PLANT\_COMMIT}(r,t-1,j)\right) \\ & + \text{ramp\_up\_rt}(j) \\ & \cdot \left(1 + \text{PLANT\_COMMIT}(r,t-1,j) - \text{PLANT\_COMMIT}(r,t,j)\right)] \\ & \cdot \text{uc\_flag}(j) + \text{ramp\_up\_rt}(j) \cdot \left(1 - \text{uc\_flag}(j)\right) \\ & + capacity\_rampup\_UB(r,t,j)\end{aligned} \quad \text{(A8)}$$

$$\begin{aligned}\forall r,t,j: & \; ramp\_down(r,t,j) + \text{SPINDOWN}(r,t,j) \\ & \leq [\text{min\_pwr\_out}(r,t,j) \\ & \cdot \left(2 - \text{PLANT\_COMMIT}(r,t,j) - \text{PLANT\_COMMIT}(r,t-1,j)\right) \\ & + \text{ramp\_down\_rt}(j) \\ & \cdot \left(1 - \text{PLANT\_COMMIT}(r,t-1,j) + \text{PLANT\_COMMIT}(r,t,j)\right)] \\ & \cdot \text{uc\_flag}(j) + \text{ramp\_down\_rt}(j) \cdot \left(1 - \text{uc\_flag}(j)\right) \\ & + capacity\_rampdown\_UB(r,t,j)\end{aligned} \quad \text{(A9)}$$

where $ramp\_up(r,t,j) = power\_out(r,t,j) - power\_out(r,t-1,j)$ and $ramp\_down(r,t,j) = power\_out(r,t-1,j) - power\_out(r,t,j)$.

The non-synchronous spin-up constraint (eq. A10) limits the reserve contribution of generation units to their maximum ramp-up capability when they are not committed to operating. It ensures that non-synchronous reserves are available only to units capable of ramping up to full capacity within a single time step and applies exclusively to units with high ramp-up rates operating under unit commitment.

$$\forall r,t,j: \text{NS\_SPINUP}(r,t,j) \leq [1 - \text{PLANT\_COMMIT}(r,t,j)] \cdot \text{ramp\_up\_rt}(j) \tag{A10}$$

The next seven constraints are related to unit commitment that collectively govern the operational decisions for dispatchable generation units. In particular, the logical constraint for unit commitments (eq. 11) establishes consistency between commitment, startup, and shutdown decisions, preventing contradictory states. Minimum up-time constraints (eq. A12-A14) ensure that once a unit is started, it remains online for its required operational duration, accounting for initial conditions, rolling horizon requirements, and end-of-horizon scenarios. Similarly, minimum down-time constraints (eq. A15-A17) enforce that once a unit is shut down, it remains offline for the mandated downtime, incorporating initial conditions, operational transitions, and end-of-horizon considerations.

$$\begin{aligned}\forall r,t,j: \text{PLANT\_COMMIT}(r,t,j) - \text{PLANT\_COMMIT}(r,t-1,j) \\ = \text{PLANT\_START}(r,t,j) - \text{PLANT\_SHUT}(r,t,j)\end{aligned} \tag{A11}$$

$$\forall r,t,j: \sum_{\text{tt} \mid tt \leq \text{G(j)}} \left(1 - \text{PLANT\_COMMIT}(r,t,j)\right) = 0 \tag{A12}$$

$$\begin{aligned}\forall r,t,j: \sum_{\text{tt} \mid \text{tt} \geq t \wedge \text{tt} \leq (t + \text{MIN\_UPTIME}(j) - 1)} \text{PLANT\_COMMIT}(r,\text{tt},j) \\ \geq \text{MIN\_UPTIME}(j) \\ \cdot [\text{PLANT\_COMMIT}(r,t,j) - \text{PLANT\_COMMIT}(r,t-1,j)]\end{aligned} \tag{A13}$$

$$\begin{aligned}\forall r,t,j: \sum_{\text{tt} \mid t \leq \text{tt} \wedge \text{tt} \leq \text{card(t)}} [\text{PLANT\_COMMIT}(r,\text{tt},j) \\ - \left(\text{PLANT\_COMMIT}(r,t,j) - \text{PLANT\_COMMIT}(r,t-1,j)\right)] \geq 0\end{aligned} \tag{A14}$$

$$\forall r,t,j: \sum_{\text{tt} \mid tt \leq \text{L(j)}} \text{PLANT\_COMMIT}(r,\text{tt},j) = 0 \tag{A15}$$

$$\begin{aligned}\forall r,t,j: \sum_{\text{tt} \mid \text{tt} \geq t \wedge tt \leq (t + \text{MIN\_DOWNTIME}(j) - 1)} \left(1 - \text{PLANT\_COMMIT}(r,\text{tt},j)\right) \\ \geq \text{MIN\_DOWNTIME}(j) \\ \cdot [\text{PLANT\_COMMIT}(r,t-1,j) - \text{PLANT\_COMMIT}(r,t,j)]\end{aligned} \tag{A16}$$

$$\begin{aligned}\forall r,t,j: \sum_{\text{tt} \mid \text{tt} \geq t \wedge tt \leq \text{card(t)}} [1 - \text{PLANT\_COMMIT}(r,\text{tt},j) \\ - \left(\text{PLANT\_COMMIT}(r,t-1,j) - \text{PLANT\_COMMIT}(r,t,j)\right)] \geq 0\end{aligned} \tag{A17}$$

Storage constraints

The next three constraints are related to modelling the operational behaviour of storage units. First, the storage charge constraint (eq. A18) prevents storage units from charging beyond their design capacity, while the storage discharge constraint (eq. A19) limits discharge rates to within defined operational capacities. The storage maximum energy constraint (eq. A20) ensures that the energy level in storage does not exceed the unit's maximum volume capacity, accounting for charging, discharging, inflows, and losses.

$$\forall r,t,j\text{: STOR\_CHRG}(r,t,j) \leq \text{stor\_chrg\_cap}(r,t,j) \cdot \left[\text{STOR\_CHRG\_COMMIT}(r,t,j) + \left(1 - \text{stor\_uc\_flag}(j)\right)\right] \quad \text{(A18)}$$

$$\forall r,t,j\text{: STOR\_DCHRG}(r,t,j) \leq \text{stor\_dchrg\_cap}(r,t,j) \cdot \left[1 - \text{STOR\_CHRG\_COMMIT}(r,t,j) \cdot \text{stor\_uc\_flag}(j)\right] \quad \text{(A19)}$$

$$\forall r,t,j\text{: storage\_level}(r,t,j) \leq \text{stor\_vol\_cap}(j),$$
where
$$\text{storage\_level}(r,t,j) = \text{storage\_level}(r,t-1,j) + \left[\text{stor\_hydro\_inflow}(r,t,j) - \text{HYDRO\_CURT}(r,t,j)\right] + \left[\text{STOR\_CHRG}(r,t,j) \cdot \left(1 - \text{eff\_loss}(j)\right) - \text{STOR\_DCHRG}(r,t,j)\right]. \quad \text{(A20)}$$

The following two constraints regulate storage's participation in spinning reserves by linking reserve contributions to charging and discharging operations. The storage spin-up constraint (eq. A21) ensures that the spinning reserve contribution during discharge does not exceed the current energy discharge rate, maintaining consistency with operational limits. Similarly, the storage spin-down constraint (eq. A22) limits the spinning reserve contribution during charging to the current charging rate, preventing over-commitment of reserve capacity.

$$\forall r,t,j\text{: STOR\_SPINUP}(r,t,j) \leq \text{STOR\_DCHRG}(r,t,j) \quad (21)$$

$$\forall r,t,j\text{: STOR\_SPINDOWN}(r,t,j) \leq \text{STOR\_CHRG}(r,t,j) \quad (22)$$

In this model, two types of DSR are considered: implicit (load shifting) and explicit (peak shaving). Both are modelled as storage technologies.

Load-shifting assumes that the storage state returns to zero at the end of each modelling horizon (see eq. A23 for more details). This assumption ensures energy neutrality for storage units modelled as implicit DSR technologies. Starting at zero energy at the beginning of the time horizon (t = 1), these units must return to zero by the end. This maintains the total energy balance across the horizon, enabling load-shifting without altering overall energy consumption.

Peak-shaving DSR, modelled as a storage unit without charging capability (with charge capacity set to zero in the input sheet), assumes daily energy response availability, defined in MWh-e/day. This availability is provided as "energy inflow" at the start of the first hour of each day. The model then optimises the timing and extent of peak-shaving activation within the daily response limits.

$$\forall r,j\text{: } \sum_{t=T_{max}} \text{storage\_level}(r,t,j) = 0 \quad \text{(A23)}$$

Fuel flow constraints

The fuel supply constraint (eq. 24) ensures that the total fuel consumption by generation technologies at a node does not exceed the maximum allowable fuel flow for that fuel type and time step. Its shadow price reflects the marginal benefit of increasing the fuel supply limit.

$$\forall r,t,f,n: \sum_{j(n)} \text{fuel\_cons\_power}(r,t,f,j) \leq \text{fuel\_flow}(r,t,f,n) \quad \text{(A24)}$$

In this model version, we also consider dual-fuel capability for individual generation units. In particular, the dual-fuel modelling framework enables generation units to operate using both primary and secondary fuels, with the secondary fuel subject to initial stock constraints. The model tracks secondary fuel use through the variable FuelStock_level (eq. A25), ensuring consumption respects the fuel stock's availability. Primary fuels with unlimited availability are modelled without an initial stock, whereas secondary fuels with limited supply require an initial stock.

$$\forall r,t,f,j: \text{FuelStock\_level}(r,t,f,j) = \text{fuel\_stock\_init}(f,j) - \text{FUEL\_CONS\_POWER}(r,t,f,j) \quad \text{(A25)}$$

External (semi-endogenous) interconnector constraints
Semi-endogenous interconnectors are a modelling construct used to represent electricity trade between fully optimised systems and systems with simplified assumptions about supply and demand (see Chyong and Newbery, 2022 who first implemented this approach in their GB UCED model). These interconnectors operate under the principle that while the electricity supply and demand balance on one side of the interconnector is fully endogenous - meaning it is optimised within the model considering all system constraints and dynamics - the other side is treated as having unlimited supply or demand capacity (a "sink") at an externally determined price.

- Imports: When the model determines that it is optimal to import electricity, it assumes an unlimited supply from the external system via the interconnector. The price at which this supply occurs is fixed exogenously, independent of the model's internal optimisation process. The model then balances how much to import at this fixed price, given its internally optimised demand and supply balance.
- Exports: Conversely, when the model chooses to export electricity, it assumes an unlimited ability to send electricity to the external system, where it is absorbed at an exogenously fixed price on the external side of the interconnector. The model then balances the marginal cost of such exports from its internally optimised market against the exogenously fixed price. If the marginal cost of internal supply resources exceeds the fixed price, export will not occur.

This approach provides a simplified representation of interconnector flow modelling, helping reduce the modelling complexity and size. By not requiring a fully endogenous representation of the external system, it becomes possible to focus computational resources on the key research questions and projects where detailed interconnection modelling is not necessary.

The following eight constraints describe in greater detail the modelling framework for the (semi-endogenous) external interconnector (IC). First, the external IC import constraint (eq. A26) ensures that electricity imports through an interconnector do not exceed its maximum power capacity, with operation contingent on the interconnector being in import mode. Its shadow price reflects the marginal benefit of increasing the import capacity. Similarly, the external IC export constraint (eq. A27) limits electricity exports to the maximum defined export capacity, enforced only when the interconnector is not in import mode. The shadow price for this constraint represents the economic value of increasing the export capacity.

$$\forall r,t,j: \text{EXT\_IC\_IMP}(r,t,j) \leq \text{max\_pwr\_out}(r,t,j) \cdot \text{EXT\_IC\_COMMIT}(r,t,j) \quad \text{(A26)}$$
$$\forall r,t,j: \text{EXT\_IC\_EXP}(r,t,j) \leq \text{min\_pwr\_out}(r,t,j) \cdot \left(1 - \text{EXT\_IC\_COMMIT}(r,t,j)\right) \quad \text{(A27)}$$

Further, to model the ramp rates and transitions between export and import for (semi-endogenous) interconnectors properly, we impose the following constraints.

- Import Ramp-Up and Ramp-Down Constraints (eqs. A28-A29): These constraints limit the increase or decrease in import flows across consecutive time steps, subject to predefined ramp rates. We assume the same ramp rate for import flow increases and decreases; hence, we use *ramp_up_rt* to represent the ramp limit on import flows.
- Export Ramp-Up and Ramp-Down Constraints (eqs. A30-A31): Similar to the import ramp rate constraints, these constraints enforce limits on the rate of change of export flows, ensuring that transitions between consecutive time steps do not exceed the interconnector's ramping capability. We assume the same ramp rate for both export flow increases and decreases; hence, we use *ramp_down_rt* to represent the ramp limit on export flows.
- Transition Ramp Constraints (eqs. A32-A33): These constraints govern the shift between export and import modes, ensuring the combined flow change does not exceed a defined transition ramp rate. This prevents abrupt shifts in flows that could potentially violate ramp rates.

$$\forall r,t,j\text{: EXT\_IC\_IMP}(r,t,j) - \text{EXT\_IC\_IMP}(r,t-1,j) \leq \text{ramp\_up\_rt}(j) \quad \text{(A28)}$$
$$\forall r,t,j\text{: EXT\_IC\_IMP}(r,t-1,j) - \text{EXT\_IC\_IMP}(r,t,j) \leq \text{ramp\_up\_rt}(j) \quad \text{(A29)}$$
$$\forall r,t,j\text{: EXT\_IC\_EXP}(r,t,j) - \text{EXT\_IC\_EXP}(r,t-1,j) \leq \text{ramp\_down\_rt}(j) \quad \text{(A30)}$$
$$\forall r,t,j\text{: EXT\_IC\_EXP}(r,t-1,j) - \text{EXT\_IC\_EXP}(r,t,j) \leq \text{ramp\_down\_rt}(j) \quad \text{(A31)}$$
$$\forall r,t,j\text{: EXT\_IC\_IMP}(r,t,j) + \text{EXT\_IC\_EXP}(r,t-1,j) \leq \text{ramp\_trans\_ext\_ic}(j), \quad \text{(A32)}$$
$$\text{where ramp\_trans\_ext\_ic(j)} = \min\big(\text{ramp\_up\_rt(j)}, \text{ramp\_down\_rt(j)}\big)$$
$$\forall r,t,j\text{: EXT\_IC\_EXP}(r,t,j) + \text{EXT\_IC\_IMP}(r,t-1,j) \leq \text{ramp\_trans\_ext\_ic}(j) \quad \text{(A33)}$$

Thus, these constraints (eqs. A28-A33) ensure the feasibility of interconnector flows adhering to the required ramp rate restrictions.

Nodal network constraints

We set up the model to allow a detailed network flow modelling, following a nodal market design and use power transfer distribution factors to model power network flows. The following three constraints describe this power flow and network modelling:

- Nodal Net Energy Injection Variable (eq. A34): This variable computes the net energy balance at each node, integrating generation, storage operations, interconnector flows, HVDC line flows, demand (including curtailment), and storage charging. It forms the basis for calculating power flows in eqs. A35 and A36.
- Nodal Forward Line Flow Constraint (eq. A35): This constraint limits forward power flow on transmission lines to their maximum allowable capacity, accounting for nodal net energy injections and Power Transfer Distribution Factors (PTDF).
- Nodal Backward Line Flow Constraint (eq. A36): This constraint similarly limits the power flow in the reverse direction to the line's maximum capacity. A relaxation variable in both eqs. A35-A36 allow for constrained violations at a penalised cost.

$$
\begin{aligned}
\forall r,t,n\text{: } & nodal\_net\_energy\_inj(r,t,n) \\
& = \sum_{j(n)} power\_out(r,t,j) \cdot \left(1 - \text{eff\_loss}(j)\right) \\
& + \sum_{j(n)} \text{STOR\_DCHRG}(r,t,j) + \sum_{j(n)} \text{ext\_ic\_net\_flow}(r,t,j) \\
& \cdot \left(1 - \text{eff\_loss}(j)\right) \\
& + \sum_{(nn,k)} \left[\text{E\_IZ\_FLOW}(r,t,nn,k,n) - \text{E\_IZ\_FLOW}(r,t,n,k,nn)\right] \\
& - \left[\text{demand\_e}(r,t,n) - \text{DEM\_E\_CURT}(r,t,n)\right] \\
& - \sum_{j(n)} \text{STOR\_CHRG}(r,t,j)
\end{aligned}
\tag{A34}
$$

$$
\begin{aligned}
\forall r,t,\text{k}\text{: } & nodal\_line\_flow(r,t,k) \\
& \leq \text{nodal\_line\_cap}(r,t,k) + \text{capacity\_line\_flow\_fw}(r,t,k),
\end{aligned}
$$

where:

$$
\begin{aligned}
& nodal\_line\_flow(r,t,k) \\
& = \sum_{n} nodal\_net\_energy\_inj(r,t,n) \cdot \text{nodal\_reduced\_PTDF}(n,k)
\end{aligned}
\tag{A35}
$$

$$
\begin{aligned}
& \text{nodal\_reduced\_PTDF}(\text{n},\text{k}) \\
& = \{0, \text{if } |\text{nodal\_PTDF}(\text{n},\text{k})| \\
& < \text{nodal\_PTDF\_cutoff}, \text{else nodal\_PTDF}(\text{n},\text{k})\}
\end{aligned}
$$

$$
\begin{aligned}
\forall r,t,k\text{: } & nodal\_line\_flow(r,t,k) \\
& \geq -\left(\text{nodal\_line\_cap}(r,t,k) + \text{capacity\_line\_flow\_bw}(r,t,k)\right)
\end{aligned}
\tag{A36}
$$

Together, these components (eqs. A34-A36) ensure a comprehensive nodal market model, maintaining a detailed power-flow representation while accounting for transmission constraints. Shadow prices from these constraints (eqs. A35-A36) provide insights into the value of increasing transmission capacity and are used to compute locational marginal prices (LMPs).

Further, in the nodal market design mode, we also include interface-level constraints to manage aggregated power flows across multiple transmission lines (eqs. A37-A38):

- Nodal Forward Interface Flow Constraint (eq. A37): This constraint limits the total forward power flow across all transmission lines within a specified interface to its maximum allowable capacity. It accounts for the directional flow of each line and allows for constraint relaxation at a penalty cost to handle infeasibilities. The shadow price reflects the economic value of increasing the interface's forward flow capacity, with high values indicating congestion.
- Nodal Backward Interface Flow Constraint (eq. A38): This constraint similarly restricts the total backward power flow across transmission lines within an interface to its maximum capacity. It ensures operational limits are respected for flows in the reverse direction, with a relaxation option for constraint violations. The shadow price indicates the value of increasing backwards-flow capacity, highlighting congestion issues when it is high.

$$
\begin{aligned}
\forall r,t,i\text{: } & \sum_{k(i)} \text{nodal\_line\_direction}(\text{k}) \cdot nodal\_line\_flow(r,t,k) \\
& \leq \text{nodal\_iface\_cap}(i) + \text{capacity\_iface\_flow\_fw}(r,t,i)
\end{aligned}
\tag{A37}
$$

$$
\begin{aligned}
\forall r,t,i\text{: } & \sum_{k(i)} \text{nodal\_line\_direction}(k) \cdot nodal\_line\_flow(r,t,k) \\
& \geq -\left(\text{nodal\_iface\_cap}(i) + \text{capacity\_iface\_flow\_bw}(r,t,i)\right)
\end{aligned}
\tag{A38}
$$

These constraints (eqs. A37-A38) ensure that interface-level power flows remain within defined limits, addressing the aggregated impacts of line capacities on network flows.

Interzonal network constraints

Similar to the way we model semi-endogenous interconnector flows (eqs. A26-A33), we describe a fully endogenous interzonal (IZ) interconnector flows approach here. The first block of constraints for fully endogenous interzonal (IZ) flow modelling ensures operational consistency (e.g., avoiding simultaneous flows in both directions), maximum flow capacity, and ramp rate for interzonal lines:

- Interzonal Flow Commitment Constraint (eq. A39): This constraint enforces that only one flow direction (either forward or backward) can be committed on an interzonal line at any given time step. This prevents simultaneous bidirectional flow commitments on line *k*.
- Interzonal Maximum Flow Constraint (eq. A40): It limits interzonal electricity flow to the dynamic capacity of the line when the flow in a specific direction is committed. This ensures that flows respect the line's capacity.
- Interzonal Flow Ramp-Up Constraint (eq. A41): This constraint restricts the rate of increase in electricity flow on interzonal lines between consecutive time steps, adhering to predefined ramp-up limits.
- Interzonal Flow Ramp-Down Constraint (eq. A42): Similarly, this constraint limits the rate of decrease in interzonal flow, enforcing predefined ramp-down limits.

$$\forall r,t,k: \sum_{(n,nn)} \text{IZFLOW\_COMMIT}(r,t,n,k,nn) \leq 1 \quad \text{(A39)}$$

$$\forall r,t,n,k,nn: \text{E\_IZ\_FLOW}(\text{r,t,n,k,nn}) \leq \left[\text{IZFLOW\_COMMIT}(\text{r,t,n,k,nn}) + \left(1 - \text{iz\_uc\_flow\_flag}(\text{n,k,nn})\right)\right] \cdot \text{iz\_line\_cap}(\text{r,t,n,k,nn}) \quad \text{(A40)}$$

$$\forall r,t,n,k,nn: \text{E\_IZ\_FLOW}(\text{r,t,n,k,nn}) - \text{E\_IZ\_FLOW}(\text{r,t}-1\text{,n,k,nn}) \leq \text{iz\_line\_ramp}(\text{n,k,nn}) \quad \text{(A41)}$$

$$\forall r,t,n,k,nn: \text{E\_IZ\_FLOW}(\text{r,t}-1\text{,n,k,nn}) - \text{E\_IZ\_FLOW}(\text{r,t,n,k,nn}) \leq \text{iz\_line\_ramp}(\text{n,k,nn}) \quad \text{(A42)}$$

These constraints (eqs. A39-A42) collectively ensure that interzonal electricity flows align with defined maximum flow capacities, directional commitments, and ramping limits.

The next block of constraints addresses the operational and transition dynamics of interzonal (IZ) flow, ensuring adherence to ramping limits and logical consistency during directional changes. The approach is based on a linearised approach involving binary variables - *FlowChange_BW_FW(r,t,k)* and *FlowChange_FW_BW(r,t,k)* - and the following constraints:

- Interzonal Transition Ramp Constraints (eqs. A43-A44): These constraints limit the magnitude of interzonal flow changes during directional transitions, limiting backwards-to-forward (eq. A43) and forward-to-backwards (eq. A44) shifts within ramping limits. They ensure that transitions respect both ramp constraints and dynamic capacity profiles.
- Flow Transition Variables for Backwards-to-Forward (eqs. A45-A47): These constraints define the binary variable *FlowChange_BW_FW(r,t,k)* to track valid transitions from backwards to forward flow. They ensure this variable activates only when flow commitments meet logical conditions for a directional transition while preventing incorrect activations.
- Flow Transition Variables for Forward-to-Backwards (eqs. A48-A50): Similar to eqs. A45-A47, these constraints define the binary variable *FlowChange_FW_BW(r,t,k)* to track valid transitions from forward to backward flow. They enforce logical activation of the variable based on flow commitments at successive time steps.

$$\forall r,t,k: \sum_{(n,nn)} \mathrm{E\_IZ\_FLOW}(r,t,n,k,nn) \cdot \mathrm{iz\_flow\_dir\_flag}(n,k,nn) + \sum_{(n,nn)} [\mathrm{E\_IZ\_FLOW}(r,t-1,n,k,nn)] \cdot (1-\mathrm{iz\_flow\_dir\_flag}(n,k,nn)) \leq \mathrm{iz\_line\_ramp\_bw\_fw}(k) \cdot \mathrm{FlowChange\_BW\_FW}(r,t,k) + \sum_{(n,nn)} \mathrm{iz\_line\_cap\_stat}(n,k,nn) \cdot \mathrm{iz\_line\_cap\_prof}(r,t,k) \cdot (1-\mathrm{FlowChange\_BW\_FW}(r,t,k)) \tag{A43}$$

$$\forall r,t,k: \sum_{(n,nn)} \mathrm{E\_IZ\_FLOW}(r,t,n,k,nn) \cdot (1-\mathrm{iz\_flow\_dir\_flag}(n,k,nn)) + \sum_{(n,nn)} [\mathrm{E\_IZ\_FLOW}(r,t-1,n,k,nn)] \cdot \mathrm{iz\_flow\_dir\_flag}(n,k,nn) \leq \mathrm{iz\_line\_ramp\_fw\_bw}(k) \cdot \mathrm{FlowChange\_FW\_BW}(r,t,k) + \sum_{(n,nn)} \mathrm{iz\_line\_cap\_stat}(n,k,nn) \cdot \mathrm{iz\_line\_cap\_prof}(r,t,k) \cdot (1-\mathrm{FlowChange\_FW\_BW}(r,t,k)) \tag{A44}$$

$$\forall r,t,n,k,nn: \mathrm{FlowChange\_BW\_FW}(r,t,k) \leq \sum_{(n,nn)} \mathrm{IZFLOW\_COMMIT}(r,t,n,k,nn) \cdot \mathrm{iz\_flow\_dir\_flag}(n,k,nn) \tag{A45}$$

$$\forall r,t,k: \mathrm{FlowChange\_BW\_FW}(r,t,k) \leq \sum_{(n,nn)} \mathrm{IZFLOW\_COMMIT}(r,t-1,n,k,nn) \cdot (1-\mathrm{iz\_flow\_dir\_flag}(n,k,nn)) \tag{A46}$$

$$\forall r,t,k: \mathrm{FlowChange\_BW\_FW}(r,t,k) \geq \sum_{(n,nn)} \mathrm{IZFLOW\_COMMIT}(r,t,n,k,nn) \cdot \mathrm{iz\_flow\_dir\_flag}(n,k,nn) + \sum_{(n,nn)} \mathrm{IZFLOW\_COMMIT}(r,t-1,n,k,nn) \cdot (1-\mathrm{iz\_flow\_dir\_flag}(n,k,nn)) - 1 \tag{A47}$$

$$\forall r,t,k: \mathrm{FlowChange\_FW\_BW}(r,t,k) \leq \sum_{(n,nn)} \mathrm{IZFLOW\_COMMIT}(r,t,n,k,nn) \cdot (1-\mathrm{iz\_flow\_dir\_flag}(n,k,nn)) \tag{A48}$$

$$\forall r,t,k: \mathrm{FlowChange\_FW\_BW}(r,t,k) \leq \sum_{(n,nn)} \mathrm{IZFLOW\_COMMIT}(r,t-1,n,k,nn) \cdot \mathrm{iz\_flow\_dir\_flag}(n,k,nn) \tag{A49}$$

$$\forall r,t,k: \mathrm{FlowChange\_FW\_BW}(r,t,k) \geq \sum_{(n,nn)} \mathrm{IZFLOW\_COMMIT}(r,t,n,k,nn) \cdot (1-\mathrm{iz\_flow\_dir\_flag}(n,k,nn)) + \sum_{(n,nn)} \mathrm{IZFLOW\_COMMIT}(r,t-1,n,k,nn) \cdot \mathrm{iz\_flow\_dir\_flag}(n,k,nn) - 1 \tag{A50}$$

Hydrogen dispatch module

The hydrogen dispatch module integrates hydrogen production, storage, transport, and utilisation within an electricity optimisation framework (Figure A. 1, taking the GB market as an example). This approach captures interactions between electricity and hydrogen flows, ensuring a comprehensive representation of hydrogen's role in energy systems. The module supports two modelling approaches - price-based and demand-based - offering flexibility to explore scenarios driven by market dynamics or predefined hydrogen demand.

Node-Based Modelling Framework

- Electricity Nodes (e.g., GB_e) handle power for hydrogen production and receive electricity generated from hydrogen-fueled technologies.
- Hydrogen Nodes (e.g., GB_h2) consolidate production, storage, and local demand, with future scope for integrating exogenous supply.
- Hydrogen Power Generation Nodes (e.g., GB_h2_PowerGen) consume hydrogen to generate electricity, which is then exported back to electricity nodes.

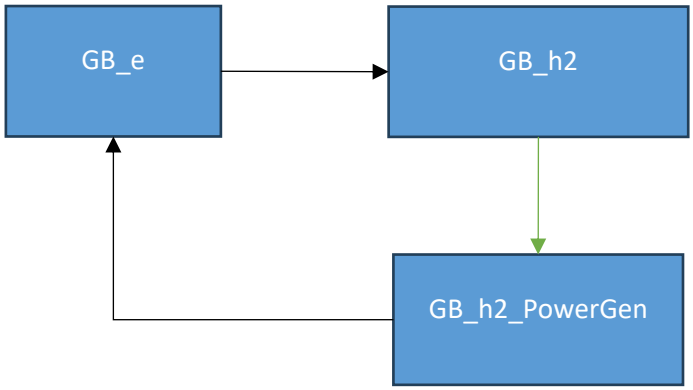

Figure A. 1: Schematic of electricity and hydrogen nodes
Notes: Black font arrows are electricity flow; Green arrows are hydrogen flow.

All in all, this hydrogen module, therefore, has eleven constraints.

Hydrogen Supply and Demand Balances

- Hydrogen Energy Balance (eq. A51): Ensures that hydrogen production, storage discharge, interzonal inflows, and demand curtailment align with node-level demand. This forms the core balance equation for hydrogen nodes, maintaining system-wide consistency.
- Electrolyser Input Balance (eq. A52): Balances electricity demand from electrolysers with electricity inflows to ensure operational feasibility and grid compatibility.
- CCGT-H2 Fuel Demand and Supply (eq. A53): Matches hydrogen consumption by hydrogen-fueled power plants with interzonal inflows, maintaining alignment between supply and demand.
- CCGT-H2 Electricity Export Balance (eq. A54): Limits electricity exports to the total generation output of hydrogen-fueled power plants, reflecting thermal efficiency and operational realism.

$$\forall r,t,n: \sum_{j(n)} H2\_output(r,t,j) + \sum_{j(n)} \text{H2\_STOR\_DCHRG}(r,t,j) + \sum_{(nn,k)} \text{H2\_IZ\_FLOW}(r,t,nn,k,n) \cdot \left(1 - \text{H2\_iz\_line\_loss}(k)\right) = \text{H2\_demand}(r,t,n) - \text{H2\_DEM\_CURT}(r,t,n) + \sum_{j(n)} \text{H2\_STOR\_CHRG}(r,t,j) + \sum_{(nn,k)} \text{H2\_IZ\_FLOW}(r,t,n,k,nn) \quad \text{(A51)}$$

$$\forall r,t,n: \sum_{j(n)} \text{H2\_ELEC\_PWR\_CONS}(r,t,j) = \sum_{(nn,k)} \text{E\_IZ\_FLOW}(r,t,nn,k,n) \quad \text{(A52)}$$

$$\forall r,t,n: \sum_{\text{f,j(n)|f=H2}} \text{FUEL\_CONS\_POWER}(r,t,f,j) = \sum_{(nn,k)} \text{H2\_IZ\_FLOW}(r,t,nn,k,n) \quad \text{(A53)}$$

$$\forall r,t,n: \sum_{(k,nn)} \text{E\_IZ\_FLOW}(r,t,n,k,nn) = \sum_{f,j(n)|f=\text{H2}} \text{FUEL\_CONS\_POWER}(r,t,f,j) \cdot \text{thermal\_eff}(f,j)) \quad \text{(A54)}$$

Electrolyser Operation Constraints

- Maximum Power Consumption (eq. A55): Sets an upper bound on electrolyser power consumption based on defined capacities.
- Ramp-Up and Ramp-Down (eqs. A56-A57): Limit the rate of increase or decrease in electrolyser power consumption.

$$\forall r,t,j: \text{H2\_ELEC\_PWR\_CONS}(r,t,j) \leq \text{H2\_elec\_cap}(r,t,j) \quad \text{(A55)}$$

$$\forall r,t,j: \text{H2\_ELEC\_PWR\_CONS}(r,t,j) - \text{H2\_ELEC\_PWR\_CONS}(r,t-1,j) \leq \text{H2\_elec\_ramp\_up}(j) \quad \text{(A56)}$$

$$\forall r,t,j: \text{H2\_ELEC\_PWR\_CONS}(r,t-1,j) - \text{H2\_ELEC\_PWR\_CONS}(r,t,j) \leq \text{H2\_elec\_ramp\_down}(j) \quad \text{(A57)}$$

Hydrogen Storage Constraints

- Charging and Discharging Capacities (eqs. A58-A59): Ensure that hydrogen storage units operate within their defined charging and discharging capacities.
- Storage Volume Capacity (eq. A60): Limits the total hydrogen volume in storage units to their maximum capacity.

$$\forall r,t,j: \text{H2\_STOR\_CHRG}(r,t,j) \leq \text{H2\_stor\_chg\_cap}(r,t,j) \quad \text{(A58)}$$

$$\forall r,t,j: \text{H2\_STOR\_DCHRG}(r,t,j) \leq \text{H2\_stor\_dchg\_cap}(r,t,j) \quad \text{(A59)}$$

$$\forall r,t,j: \text{H2\_Storage\_level}(r,t,j) \leq \text{H2\_stor\_vol\_cap}(j) \quad \text{(A60)}$$

Hydrogen Transport Constraint (eq. A61) caps interzonal hydrogen flows at pipeline capacities.

$$\forall r,t,n,k,nn: \text{H2\_IZ\_FLOW}(r,t,n,k,nn) \leq \text{H2\_iz\_line\_cap}(r,t,n,k,nn) \quad \text{(A61)}$$

With this approach, there are two methods for modelling hydrogen dispatch:

1. **Hydrogen Price-Based Method**
   In this approach, hydrogen production via electrolysis is driven by the cost dynamics of electricity (endogenously determined in the model) and by an assumed hydrogen price and the variable cost of electrolysis, both of which are model inputs. The model endogenously determines electricity costs, balancing these against the hydrogen price and the variable operating cost of electrolysis. Hydrogen is produced if the assumed hydrogen price is sufficiently high to offset the variable electrolysis costs and any associated electricity production costs.
   This method also accounts for surplus electricity scenarios, particularly from near-zero-marginal-cost resources such as wind and solar. When electricity prices approach zero due to the potential curtailment of renewables, electrolysis will likely be activated to convert the surplus electricity into hydrogen.
   This method provides flexibility to simulate hydrogen production in response to market conditions, aligning electrolysis activity with renewable electricity availability and cost dynamics.
2. **Traditional Demand-Based Method**
   In this more conventional approach, hydrogen demand is treated as an input that must be satisfied. The model enforces hydrogen production to meet the specified demand, irrespective of hydrogen price, variable electrolysis costs, or electricity costs. This is achieved by setting a very high hydrogen curtailment cost, effectively compelling the model to prioritise hydrogen production.
   However, if the hydrogen curtailment cost is low, the model may curtail demand instead, depending on electricity costs. For instance, high electricity costs could lead to reduced hydrogen production unless there is significant renewable electricity curtailment, in which case production is more likely.
   This method reflects a scenario in which hydrogen demand is non-negotiable (e.g., industrial or policy-driven targets), ensuring the model meets predefined requirements across various cost conditions.

The **price-based method** offers a market-driven approach to hydrogen production. It simulates scenarios in which production responds to electricity market conditions and to assumed hydrogen prices. It is ideal for exploring scenarios where surplus renewable energy and fluctuating costs influence hydrogen output. In contrast, the **demand-based method** prioritises meeting specific hydrogen demand, aligning with scenarios where hydrogen supply must be ensured, such as industrial processes or strategic energy planning targets. Both approaches can be adapted to include hydrogen storage and transmission to other markets, thereby enhancing system flexibility and optimising hydrogen integration within power systems.

Objective Function

Subject to the abovementioned constraints, the objective function seeks to minimise the total system cost of meeting electricity and hydrogen demand. This is achieved by optimising operational costs (fuel, carbon, variable, and fixed), incorporating penalties for constraint violations (via artificial variables), and accounting for interzonal flow and reserve operation costs. Additionally, the objective accounts for revenue from hydrogen sales if modelled as price-based hydrogen dispatch. This section first details the total system cost function to be minimised. Then, its components.

$$
\begin{aligned}
\text{MIN F} = & \sum_{(r,t,f,j,n)} FuelCost(r,t,f,j,n) + \sum_{(r,t,f,j,n)} CarbonCost(r,t,f,j,n) \\
& + \sum_{(r,t,j,n)} VariableCost(r,t,j,n) + \sum_{(r,t,j,n)} FixedCost(r,t,j,n) \\
& + \sum_{(r,t,j,n)} RampCost(r,t,j,n) + \sum_{(r,t,j,n)} ReserveCost(r,t,j,n) \\
& + \sum_{(r,t,n,k,nn)} ZonalFlowCost(r,t,n,k,nn) \\
& + \sum_{(r,t,n)} DemandCurtailmentCost(r,t,n) \\
& - \sum_{(r,t,j,n)} HydrogenRevenue(r,t,j,n) \\
& + \sum_{(r,t,n)} PenaltyReserveCost(r,t,n) \\
& + \sum_{(r,t,j,n)} PenaltyBoundCost(r,t,j,n) \\
& + \sum_{(r,t,k)} PenaltyLineFlowCost(r,t,k) \\
& + \sum_{(r,t,i)} PenaltyInterfaceCost(r,t,i)
\end{aligned}
\tag{A62}
$$

Components of the Objective Function:

Fuel Cost (*FuelCost(r,t,f,j,n)*): Represents the cost associated with fuel consumption for generation at node n for technology j using fuel f at time t.

$$
\begin{aligned}
\forall r,t,f,j,n\text{: FuelCost}(r,t,f,j,n) & \\
= ext\_ic\_net\_flow(r,t,j(f,n)) \cdot \text{fuel\_cost}(r,t,f) & \\
+ \text{FUEL\_CONS\_POWER}(r,t,f,j(n)) \cdot \text{fuel\_cost}(r,t,f) &
\end{aligned}
\tag{A63}
$$

Carbon Cost (*CarbonCost(r,t,f,j,n)*): This function captures the cost of carbon emissions for generation at node n for technology j using fuel f at time t.

$$
\begin{aligned}
\forall r,t,f,j,n\text{: CarbonCost}(r,t,f,j,n) & \\
= \text{FUEL\_CONS\_POWER}(r,t,f,j(n)) \cdot \text{thermal\_eff}(f,j) & \\
\cdot \text{carbon\_price}(r,t,n) \cdot \text{carbon\_intensity}(f,j) &
\end{aligned}
\tag{A64}
$$

Variable Cost (*VariableCost(r,t,j,n)*): Accounts for operational and maintenance costs dependent on the power and hydrogen output of technology j at node n and time t.

$$\forall r,t,f,j,n: VariableCost(r,t,j,n) = \text{varcost}(r,t,j) \cdot \left(power\_out(r,t,j(n)) + \text{STOR\_DCHRG(r,t,j(n))} + ext\_ic\_net\_flow(r,t,j(n))\right) + \text{H2\_varcost}(r,t,j) \cdot \text{H2\_STOR\_DCHRG}(r,t,j(n)) \quad \text{(A65)}$$

Fixed Cost (*FixedCost(r,t,j,n)*): This function captures fixed operational costs independent of generation levels, including cycling costs associated with starting up and shutting down technologies.

$$\forall r,t,j,n: FixedCost(r,t,j,n) = \left(\text{PLANT\_START}(r,t,j(n)) \cdot \text{start\_cost}(j) + \text{PLANT\_SHUT}(r,t,j(n)) \cdot \text{shut\_cost}(j)\right) \quad \text{(A66)}$$

Ramp Cost (*RampCost(r,t,j,n)*): Represents costs incurred due to ramping up or down generation levels.

$$\forall r,t,j,n: RampCost(r,t,j,n) = \left(ramp\_up(r,t,j(n)) \cdot \text{ramp\_up\_cost}(j) + ramp\_down(r,t,j(n)) \cdot \text{ramp\_down\_cost}(j)\right) \quad \text{(A67)}$$

Reserve Cost (*ReserveCost(r,t,j,n)*): This function reflects costs for maintaining spinning or non-spinning reserve capacities. It quantifies the economic burden of ensuring grid stability through spinning reserve contributions from various technologies, including storage systems. This helps account for reliability costs in overall system operation.

$$\forall r,t,j,n: ReserveCost(r,t,j,n) = \left(\text{NS\_SPINUP}(r,t,j) + \text{SPINUP}(r,t,j) + \text{STOR\_SPINUP}(r,t,j)\right) \cdot \text{spin\_up\_cost}(j) \quad \text{(A68)}$$

Zonal Flow Cost (*ZonalFlowCost(r,t,n,k,nn)*): This variable represents costs associated with interzonal electricity and hydrogen flows across lines *k* between nodes *n* and *nn*. By factoring in variable costs for each flow type, this variable ensures the model appropriately accounts for the potential economic impact of transporting energy resources across zones.

$$\forall r,t,n,k,nn: ZonalFlowCost(r,t,n,k,nn) = \text{E\_IZ\_FLOW}(r,t,n,k,nn) \cdot \text{iz\_line\_varcost}(n,k,nn) + \text{H2\_IZ\_FLOW}(r,t,n,k,nn) \cdot \text{H2\_iz\_line\_varcost}(n,k,nn) \quad \text{(A69)}$$

Demand Curtailment Cost (*DemandCurtailmentCost(r,t,n)*): This variable calculates the penalty costs associated with unmet electricity and hydrogen demand. The model incentivises supply-side

solutions by assigning high costs to demand curtailment, ensuring that demand is met where feasible and economically justifiable.

$$\begin{aligned}\forall r,t,n\colon\ & DemandCurtailmentCost(r,t,n)\\ &= \text{demand\_curt\_cost}(n)\cdot \text{DEM\_E\_CURT}(r,t,n)\\ &+ \text{h2\_demand\_curt\_cost}(n)\cdot \text{H2\_DEM\_CURT}(r,t,n)\end{aligned} \tag{A70}$$

Hydrogen Revenue (*HydrogenRevenue(r,t,j,n)*): Represents revenue from selling hydrogen, subtracted from the total cost to reflect income. This variable calculates the revenue generated from hydrogen sales, factoring in the market price and variable production costs. The net revenue contributes to the overall objective function by offsetting system costs, reflecting the economic benefits of hydrogen production and sales.

$$\begin{aligned}\forall r,t,j,n\colon\ & HydrogenRevenue(r,t,j,n)\\ &= \text{H2\_output}\big(r,t,j(n)\big)\cdot\big(\text{H2\_price}(r,t,n)-\text{H2\_varcost}(r,t,j)\big)\end{aligned} \tag{A71}$$

Penalty Reserve Cost (*PenaltyReserveCost(r,t,n)*): Penalty cost for violating reserve requirements at node n.

$$\begin{aligned}\forall r,t,n\colon\ & PenaltyReserveCost(r,t,n)\\ &= \text{capcost\_res\_up}(\text{n})\cdot capacity\_res\_up(r,t,n)\\ &+ \text{capcost\_res\_down}(\text{n})\cdot capacity\_res\_down(r,t,n)\end{aligned} \tag{A72}$$

Penalty Bound Cost (*PenaltyBoundCost(r,t,j,n)*): Penalty cost for exceeding generation capacity bounds for technology j at node n. This variable quantifies the penalties for violating operational constraints such as lower and upper power bounds and ramp-up and ramp-down limits.

$$\begin{aligned}\forall r,t,j,n\colon\ & PenaltyBoundCost(r,t,j,n)\\ &= \big[capacity\_power\_LB\big(r,t,j(n)\big)\cdot \text{capcost\_LB}(\text{j})\\ &+ capacity\_power\_UB\big(r,t,j(n)\big)\cdot \text{capcost\_UB}(\text{j})\\ &+ capacity\_rampup\_UB\big(r,t,j(n)\big)\cdot \text{capcost\_rampup}(\text{j})\\ &+ capacity\_rampdown\_UB\big(r,t,j(n)\big)\cdot \text{capcost\_rampdown}(\text{j})\big]\end{aligned} \tag{A73}$$

Penalty Line Flow Cost (*PenaltyLineFlowCost(r,t,k)*): Penalty cost for violating line flow constraints on line k. This variable captures the cost penalties for exceeding the transmission flow limits in either direction on a line. It ensures the model accounts for such violations and balances the trade-off between penalty flow capacity costs and feasible power flows.

$$\begin{aligned}\forall r,t,k\colon\ & PenaltyLineFlowCost(r,t,k)\\ &= \text{capcost\_line\_flow}(k)\\ &\cdot\big(capacity\_line\_flow\_fw(r,t,k)+capacity\_line\_flow\_bw(r,t,k)\big)\end{aligned} \tag{A74}$$

Penalty Interface Cost (*PenaltyInterfaceCost(r,t,i)*): Penalty cost for violating interface flow constraints on interface i.

$$\forall r, t, i: PenaltyInterfaceCost(r, t, i) = \text{capcost\_iface\_flow}(i) \cdot \left(capacity\_iface\_flow\_fw(r, t, i) + capacity\_iface\_flow\_bw(r, t, i)\right) \quad \text{(A75)}$$